NASA CONTRACTOR REPORT

NASA CR-960

NASA CR-960

MEASUREMENT OF TURBULENT CORRELATIONS IN A COAXIAL FLOW OF DISSIMILAR FLUIDS

by Gerard J. D'Souza, Anthony Montealegre, and Herbert Weinstein

Prepared by
ILLINOIS INSTITUTE OF TECHNOLOGY
Chicago, Ill.
for

NATIONAL AERONAUTICS AND SPACE ADMINISTRATION • WASHINGTON, D. C. • JANUARY 1968

NASA CR-960

MEASUREMENT OF TURBULENT CORRELATIONS IN A COAXIAL FLOW OF DISSIMILAR FLUIDS

By Gerard J. D'Souza, Anthony Montealegre, and Herbert Weinstein

Prepared under Grant No. NsG-694 by
ILLINOIS INSTITUTE OF TECHNOLOGY
Chicago, Ill.

for

NATIONAL AERONAUTICS AND SPACE ADMINISTRATION

For sale by the Clearinghouse for Federal Scientific and Technical Information
Springfield, Virginia 22151 – CFSTI price $3.00

FOREWORD

Research related to advanced nuclear rocket propulsion is described herein. This work was performed under NASA Grant NsG-694 with Mr. Maynard F. Taylor, Nuclear Systems Division, NASA Lewis Research Center as Technical Manager.

ABSTRACT

The importance of coaxial jet flows has led to much investigation in the field. In this work axial turbulence intensities in a coaxial flow of dissimilar gases are presented. The system consisted of a circular freon 12 stream issuing into a faster and much larger air stream. The air - freon 12 density ratio is 1/4. The velocity ratios ranged from 40:1 to 5:1 with an absolute air velocity not exceeding 56.0 ft / sec. The system is assumed to be incompressible and no appreciable temperature variation was observed. Measurements were made with hot-film anemometers. An aspirator probe and a parallel film probe were used. These probes were controlled by two independent constant temperature channels.

The magnitude of the axial turbulence intensities depends much on the velocity ratio of the streams. It is usually found to have a maximum value at some point between the centerline and the radius of the inner jet and then diminish to the free stream turbulence intensity. For most of the runs this maximum turbulence intensity was between 40-45% in the initial mixing region and from 10% - 15% in the "similarity region". The free stream turbulence was about 3%. In the two cases of high air - freon velocity ratio a maximum turbulence intensity of 70% was obtained in the initial mixing region. This maximum is close to the centerline. Measurements were taken at a number of axial positions, including some very close to the jet inlet. The closest was 1/3 diameter downstream and the farthest 11 diameters.

Density fluctuations were also measured but these are shown to be damped by the measuring device. Values of the correlation between velocity and density fluctuations obtained are not valid and hence are not presented, as the damped density fluctuations affect this quantity considerably.

A comparison is made between axial turbulence intensities for the heterogeneous case and those for the homogeneous case available in the literature.

TABLE OF CONTENTS

LIST OF ILLUSTRATIONS

LIST OF SYMBOLS

Symbol	Definition
A	Constant in the hot-wire anemometer equation
B	Constant in the hot-wire anemometer equation
d	Diameter of wire
l	Length of wire
P	Power input to sensor
p	Fluctuating power
r	Radius - distance from the centerline
R	Wire resistance
T. t	Time
T_x	Temperature
T_{xy}	Shearing Stress
u	Component of velocity along the flow field
U	Reference velocity
v	Component of velocity perpendicular to the flow field
V	Normal velocity past the sensor
Nu	Nusselt Number
Pr	Prandtl Number
Re	Reynolds Number
ϵ	Eddy viscosity
μ	Molecular viscosity
ρ	Density
θ	Temperature

Subscripts

1	Component 1
2	Component 2
x	x component
y	y component

Superscripts

-	Time average
′	Fluctuating component
(t)	Turbulent

CHAPTER I

INTRODUCTION

The phenomena of coaxial flow mixing of parallel streams occurs in many practical situations today. The development and wide use of ejectors, jet pumps, after burners, combustion chambers, plasma injection systems and lately, the gaseous core nuclear rocket have led to extensive investigations of the coaxial jet. A jet entering a quiescent fluid through a small aperture is called a free jet. If the outer stream is also moving, it is referred to as a compound jet. The jet is classified as homogeneous or heterogeneous depending on whether the two streams are similar or not.

Previous investigators have worked with heated and isothermal homogeneous free jets, heated and isothermal homogeneous compound jets and heterogeneous free and compound jets. Schlichting[1] and Andrade[2] were perhaps the first to present solutions for the free jet. Their work, however, was restricted to laminar jets and hence, was of academic importance only. Since then, investigations have been confined to the more important turbulent jet. These include similarity solutions for average velocities and concentrations in the flow field, determination of shear stresses, and subsequent estimation of the eddy viscosity. Both analytical and experimental work were done in this area. More recent presentations include turbulence measurements in the jet mixing region, axial and radial turbulence intensities in a homogeneous compound jet and temperature and concentration fluctuations in a free jet.

The object of this work is to present axial turbulence intensities in a heterogeneous compound jet. Figure 1.1 represents the flow system. A circular freon stream flowed into a large faster moving air stream which could be considered of infinite extent. A solid boundary separated the two fluids until the point of initial mixing. The flow was always in the very low subsonic range and assumed to be isothermal and incompressible. The instrumentation consisted of hot-film anemometers,

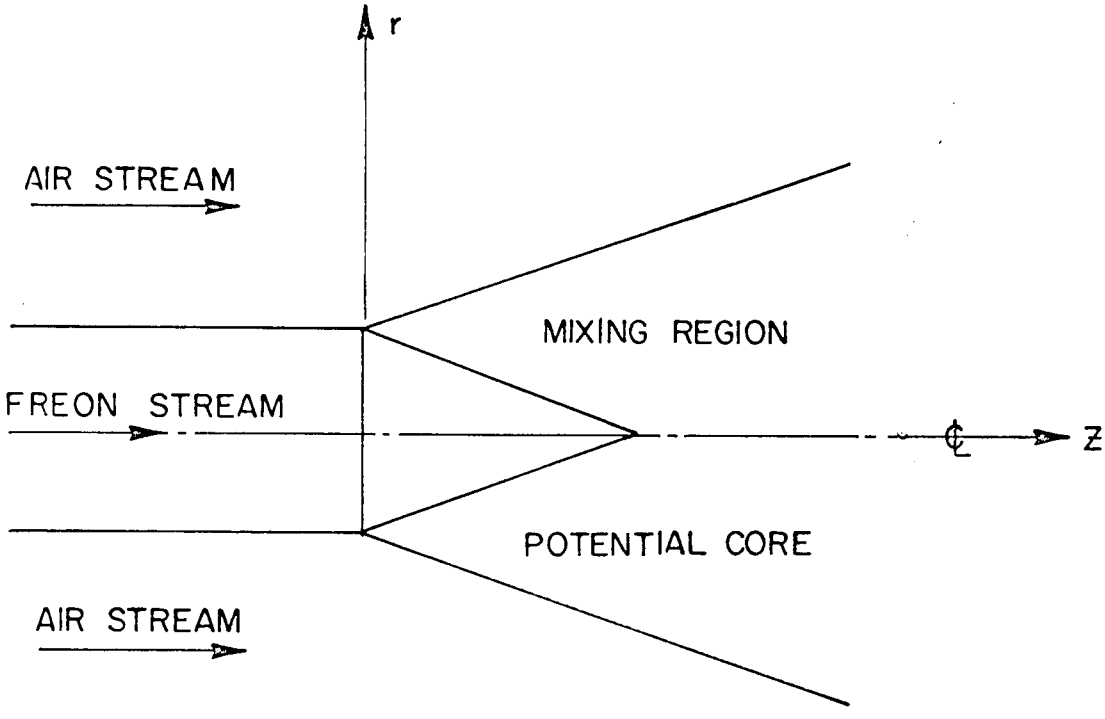

FIGURE 1.1 FLOW SYSTEM

two constant temperature control channels, a digital and an RMS voltmeter and a sum and difference unit. The hot-film anemometers used were an asiprator probe and a parallel wire probe.

An attempt was made to measure concentration fluctuations in the field. The measuring device, however, damped out these fluctuations considerably and this was detected by the resulting impossible values of the correlation. Chapter VI discusses this as well as a comparison of the homogeneous turbulence intensity data of Zawacki[3].

The air-freon density ratio is 1/4. The velocity ratios ranged from 5 to 1 to 40 to 1. The outer air stream velocity was always greater than the inner freon stream velocity. The maximum air velocity was 56 ft/sec with an initial turbulence intensity of about 3%. It is assumed that measurements made with a constant temperature hot-film anemometer are good for the turbulence intensities in the flow field.

CHAPTER II

BACKGROUND

Considerable investigation on the mixing of coaxial streams has already been made and yet very little basic information on the turbulence is available. A very brief review of these past investigations, with special reference to measurements of turbulent quantities will be presented in this chapter.

It has been shown experimentally that in turbulent flows the resultant transfer of mass heat and momentum is far greater than that of molecular transfer. Hence a majority of the investigations are confined to turbulent flows. These are characterized by a random fluctuating flow superimposed on a time smoothed mean flow. The instantaneous velocity components, pressure and density can be expressed in terms of a time-averaged mean quantity and a fluctuating quantity in the following manner.

$$U = \overline{U} + u' \qquad V = \overline{V} + v' \qquad \rho = \overline{\rho} + \rho' \qquad P = \overline{P} + p'$$

The average term denoted by the barred quantity is defined by taking a time average of the instantaneous component over a time interval T. This time T is large compared to the time scale of turbulence but small enough to detect slow variations or unsteadiness in the mean flow. For a general component Q therefore

$$\overline{Q} = \frac{1}{T} \int_{t}^{t+T} Q \, dt$$

and

$$\overline{Q'} = \frac{1}{T} \int_{t}^{t+T} Q' \, dt = 0 .$$

While the time average of any one fluctuating quantity is zero, the time average of a product of two fluctuating quantities is not necessarily zero and in fact is zero only if the two quantities are completely independent of each other.

- Concepts:

For pure laminar flow the shearing stress T_{zr} is given by

$$T_{zr} = \mu \frac{\partial u}{\partial r}$$

where μ is the molecular viscosity and $\frac{\partial u}{\partial r}$ the radial velocity gradient.

In 1887, T.V. Boussinesq studying the turbulent free jet, introduced for the first time an analogy between the turbulent shear stresses and the laminar sheer stress. He defined the turbulent shear stress T^t_{zr} as the product of the time smoothed radial velocity gradient and a turbulent transport coefficient A_t, called the eddy viscosity.

$$T^t_{zr} = A_t \frac{\partial \overline{u}}{\partial r}$$

This turbulent viscosity A_t, unlike the molecular viscosity μ, is not a property of the fluid, but instead, is dependent upon the local nature of flow. An apparent kinematic viscosity ϵ for turbulent flow is defined as $\epsilon = \frac{A_t}{\rho}$. To determine a relationship between eddy viscosity and the flow field, emperical mechanisms of turbulent transport were put forward. Among the most common and widely used theories are Prandtl's old and new mixing length theories, Taylor's hypothesis and Reichardt's[4] theory.

Many of the investigators in the field of turbulent jets were involved with determining a value for the eddy viscosity A_t. Others studied the mixing characteristics of the streams either analytically by using one of the four emperical transport mechanisms or by experimental measurements. Systems and situations varied from investigation to investigation as did experimental techniques. A few of the investigators are, Tollmein[5], Goertler[6], Kenthe[7], Squire and Trouncer[8], Ferri et al[9], Alpinieri[10], Ragsdale[11], Boehman[12] and Weinstein[13].

Corrsin[14] appears to be the first to report any fluctuating data on the round free jet. He measured turbulence intensities in a homogeneous jet with a hot wire anemometer and later with Uberoi[15] reported temperature fluctuations in a hot jet.

Tani and Kobashi[16] reported measurements of turbulent quantities for homogeneous coaxial flow in 1951. Their apparatus consisted of a 9 mm dia. jet exhausting into a tunnel 60 cm x 60 cm. With a hot wire anemometer they measured turgulence intensities in the axial ($\sqrt{u'^2}$) and radial ($\sqrt{v'^2}$) directions and the turbulent Reynolds stress $\overline{u'v'}$. They presented curves of each quantity versus a dimensionless radius, for various axial positions, all well downstream from the jet mouth. They noted that the maximum axial turbulence intensity $\sqrt{u'^2}$ occured at the maximum turbulent shear. The $\sqrt{v'^2}$ curve had no such extremities. In a contuination of the work Kobashi[17] in 1952 reported temperature fluctuation measurements of a hot free jet. taken with a single wire anemometer. He reported curves of fluctuating temperature $\sqrt{\theta'^2}$, $\sqrt{u'^2}$ and the correlation $\overline{u'\theta'}$ versus dimensionless radius. The temperature fluctuations had a local maxima, and he concluded that these fluctuations were associated with the axial velocity fluctuations. He also reported no simalirity property in the velocity fluctuations.

Zawacki[3] working with coaxial homogeneous constant temperature turbulent jets has also reported turbulent quantities $\frac{\sqrt{u'^2}}{\overline{U}}$, $\frac{\sqrt{v'^2}}{\overline{U}}$ and $\frac{\overline{u'v'}}{\sqrt{u'^2}\sqrt{v'^2}}$. His apparatus consisted of a 3/4" dia. jet in an 8" x 8" duct. Measurements were made by single and X hot film anemometers. He took measurements at various axial positions, close to the nozzle as well as far downstream. Rosensweig[18] used an optical technique to measure concentration fluctuations in a smoky jet.

Blackshear and Fingerson[19] also have reported concentration fluctuation measurements in a free jet. They used a helium jet issuing from a 1.27 cm orifice into room air as the medium. Measurements were taken with an orifice or aspirator

probe, described in Chapter IV. These were made 15 diameters away from the orifice.

It is shown in Chapter VI that concentration fluctuations measured by an aspirator probe are definitely damped by the tube and are therefore not of the same magnitude as fluctuations in the flow field.

Conger[20] used a closed system wind tunnel and hot wire anemometers to measure concentration and velocity fluctuations. He assumed that because of the nature of the setup there was isotropic turbulence and therefore no correlation of velocity to density or temperature. He could thus use a parallel wire anemometer and separate the velocity and concentration fluctuations.

CHAPTER III

ANALYTICAL

III - 1 Hot-wire Anemometer Techniques

III - 1 - 1 Fundamental Relationships

Heat transfer from small heated cylinders was first studied extensively in connection with hot-wire anemometry by King[21]. Many other investigations of the problem have been undertaken since (22, 23, 24). It is well established that the heat transferred from a hot sensor can be represented by an expression of the form

$$P = \left[A + BV^n \right] \left[T_s - T_e \right] \qquad \text{III - 1 - 1.1}$$

where A and B are numerical constants, V is the normal velocity past the sensor, T_s is the temperature of the sensor, T_e the temperature of the environment, and P the power required to maintain the sensor at the temperature T_s. The constant n is usually taken to be 1/2. An equation of this form adequately describes the power input versus velocity characteristics for hot-wire anemometers so long as the velocity is sufficiently high. If the velocity is low, below one foot per second, the power input versus square root of velocity curve is non-linear.

Each investigator's results may be put into the form of equation III-1-1.1. The difference in the analyses lies in the expressions for the constants A and B. The following emperical relationship describing the heat transfer was given by Kramers[23] and is widely used.

$$Nu = 0.42\ Pr^{0.2} + 0.57\ Pr^{1/3}\ Re^{0.5} \qquad \text{III - 1 - 1 - 1.2}$$

where Nu is the Nusselt number, Pr is the Prandtl number, and Re is the Reynolds number. The constants A and B are given by

$$A = \frac{0.42\, e\, \bar{\Lambda}\, k_f}{\alpha_1 R} \frac{l}{} (Pr)_f^{0.20} \qquad \text{III - 1 - 1.3}$$

$$B = \frac{0.57\, e\, \bar{\Lambda}\, k_f}{\alpha_1 R_o} \frac{l}{} (Pr)_f^{1/3} \left(\frac{\rho_f\, d}{\mu_f} \right)^{0.5} \qquad \text{III - 1 - 1.4}$$

and e is the conversion constant, k the thermal conductivity, μ the viscosity, ρ the density, α_1 the linear temperature coefficient of electrical resistivity, R_o the wire resistance at a reference temperature T_o, l the wire length, d the wire diameter and the subscript f means the entity is evaluated at the film temperature. The film temperature is taken as an arithmetic average of the sensor temperature, T_s and the environment temperature T_e. Thus the constants A and B depend on the physical properties of the surrounding medium as well as the dimensions of the wire.

In practice, A and B were experimentally determined for air and other freon-air mixtures. It was possible to calculate the equivalent length and diameter of the sensor from a pure air calibration and equations III-1-1.3 and III-1-1.4 and then estimate A and B for other gas mixtures by comparing physical properties. This estimate, however, was not accurate enough and the constants, A and B, were calculated for various freon-air mixtures from equation III-1-1.1. Graphs of A and B versus gas density were drawn.

The real utility, however, of hot-wire anemometers is in the measurement of turbulent properties such as turbulence intensity and turbulent shearing stress. The velocity past the sensor V is assumed to be made up of an average stream velocity U and fluctuating components u′ and v′ in the flow direction and perpendicular to the flow direction respectively.

Thus

$$V = \sqrt{(U + u')^2 + v'^2} \qquad \text{III - 1 - 1.5}$$

The quantity V^n may be expanded in a Taylor series to give

$$V^n = U^n \left[1 + n \frac{u'}{U} + \frac{n(n-1)}{2} \frac{u'^2}{U^2} + \frac{n}{2} \frac{v'^2}{U^2} + \cdots \right] \qquad \text{III - 1 - 1.6}$$

with the assumptions

$$u' << U$$

$$v' << U \qquad \text{III - 1 - 1.7}$$

Equation III-1-1.6 may be linearized to give

$$V^n = U^n \left[1 + n \frac{u'}{U} \right] \qquad \text{III - 1 - 1.8}$$

This expression may then be substituted into equation III-1-1.1 to give the instantaneous power supplied to the sensor

$$P = \overline{P} + P = \left[A + BU^n \left(1 + n \frac{u'}{U} \right) \right] \left[T_s - T_e \right] \qquad \text{III - 1 - 1.9}$$

where $\overline{P}$ is the average power level and p is the small variation about the average power level caused by the fluctuating velocity u'. The average power level $\overline{P}$ is defined as

$$\overline{P} = \left[A + B U^n \right] \left[T_s - T_e \right] \qquad \text{III - 1 - 1.10}$$

and the power level at zero velocity P_o is defined by

$$P_o = A \left[T_s - T_e \right] \qquad \text{III - 1 - 1.11}$$

Equations III-1-1.9, III-1-1.10, and III-1-1.11 may be combined to give

$$\frac{p/n}{\overline{P} - P_o} = \frac{u'}{U} \qquad \text{III - 1 - 1.12}$$

Since the average values of p and u' are zero, the root mean square (rms) values are normally used as a measure of turbulence. Defining u'^2 as the root mean square value of u' and p^2 as the root mean square value of p, equation III-1-1.12 may be written for a constant density gas

$$\frac{\sqrt{p^2}}{\overline{P} - P_o} = \frac{\sqrt{u'^2}}{U} \qquad \text{III - 1 - 1.13}$$

The quantity on the right hand side of this equation is known as the turbulence intensity. Thus, the turbulence intensity of the fluctuating component of the velocity in the mean flow direction may be easily calculated from this relationship.

Equation III-1-1.12 may be obtained in a different manner. Differentiating equation III-1-1.1 for constant density gives

$$dP = nBV^{n-1}\, dV\, (T_s - T_e) \qquad \text{III - 1 - 1.4}$$

Assuming that the fluctuating power p and the fluctuating velocity u' may be substituted for dP and dV respectively and using equations III-1-1.5 and III-1-1.7, equation III-1-1.14 may be written

$$p = \frac{nB\underline{U}^n}{U}\, u'\, (T_s - T_e) \qquad \text{III - 1 - 1.15}$$

This equation may then be combined with equations III-1-1.10 and III-1-1.11 to give equation III-1-1.12. The reason that two methods of deriving this equation are given here is that the first method shows that the turbulence intensity calculated

from this equation is for the fluctuating velocity in the mean flow direction while the second method of derivation is somewhat simpler and will be used in connection with turbulence measurements in a heterogeneous system.

If the composition of the fluid flowing past the hot-wire is variable, then the quantities A and B in equation III-1-1.1 will no longer be constant since they depend on the physical properties of the surrounding medium. The power input to the hot-wire will depend upon the concentration C or the density ρ as well as the velocity past the sensor. The total derivative of the power input to the sensor may be written

$$dP = \left(\frac{\partial P}{\partial \rho}\right)_V d\rho + \left(\frac{\partial P}{\partial V}\right)_\rho dV . \qquad \text{III - 1 - 1.16}$$

Differentiation of equation III-1-1.1 for a variable density shows that

$$\left(\frac{\partial P}{\partial \rho}\right)_V = \left[\frac{dA}{d\rho} + V^n \frac{dB}{d\rho}\right] (T_s - T_e)$$

$$\left(\frac{\partial P}{\partial V}\right)_\rho = nBV^{n-1} (T_s - T_e) \qquad \text{III - 1 - 1.17}$$

Substituting the fluctuating power p, the fluctuating velocity u' and the fluctuating density ρ' for dP, dV and $d\rho$ respectively and combining equations III-1-1.17, III-1-1.16, III-1-1.5 and III-1-1.7 gives

$$p = R' \rho' + S' u' \qquad \text{III - 1 - 1.18}$$

where

$$R' = \left[\frac{dA}{d\rho} + V^n \frac{dB}{d\rho}\right]\left[T_s - T_e\right] \qquad \text{III - 1 - 1.19}$$

and

$$S' = nBV^{n-1} (T_s - T_e) . \qquad \text{III - 1 - 1.20}$$

Dividing equation III-1-1.18 by $(T_s - T_e)$ we get

$$P' = M\rho' + Nu' \qquad \text{III - 1 - 1.21}$$

where

$$P' = \frac{P}{(T_s - T_e)}, \quad M = \frac{R'}{(T_s - T_e)}, \quad N = \frac{S'}{(T_s - T_e)} \qquad \text{III - 1 - 1.22}$$

Squaring equation III-1-1.21 and averaging we see that

$$\overline{(P')^2} = M^2 \overline{\rho'^2} + 2MN\overline{\rho'u'} + N^2 \overline{u'^2} \qquad \text{III - 1 - 1.23}$$

Affixing the subscript 1 for the first film and 2 for the other film, equation III-1-1.21 can be rewritten for each of the sensors as

$$P_1' = M_1 \rho' + N_1 u' \qquad \text{III - 1 - 1.24}$$

$$P_2' = M_2 \rho' + N_2 u' \qquad \text{III - 1 - 1.25}$$

The sum and difference of the two signals are

$$(P_1' + P_2') = (M_1 + M_2)\rho' + (N_1 + N_2)u' \qquad \text{III - 1 - 1.26}$$

$$(P_1' - P_2') = (M_1 - M_2)\rho' + (N_1 - N_2)u' \qquad \text{III - 1 - 1.27}$$

Squaring equations III-1-1.25, III-1-1.26 and III-1-1.27 and averaging,

$$\overline{P_1'^2} = M_1^2 \overline{\rho'^2} + 2M_1N_1\overline{\rho' u'} + N_1^2 \overline{u'^2} \qquad \text{III - 1 - 1.28}$$

$$\overline{P_2'^2} = M_2^2 \overline{\rho'^2} + 2M_2N_2\overline{\rho' u'} + N_2^2 \overline{u'^2} \qquad \text{III - 1 - 1.29}$$

$$\overline{(P_1' + P_2')^2} = (M_1+M_2)^2 \overline{\rho'^2} + 2 (M_1 + M_2) (N_1 + N_2) \overline{\rho' u'} + (N_1+N_2)^2 \overline{u'^2}$$

III - 1 - 1.30

$$\overline{(P_1' - P_2')^2} = (M_1 - M_2)^2 \overline{\rho'^2} + 2 (M_1 - M_2)(N_1 - N_2) \overline{\rho' u'} + (N_1-N_2)^2 \overline{u'^2}$$

III - 1 - 1.31

In the set of independen equations III-1-1.28 to III-1-1.31, we have the unknown variables $\overline{\rho'^2}$, $\overline{\rho' u'}$ and $\overline{u'^2}$. The quantities M_1, M_2, N_1, N_2, P_1', P_2', $(P_1' + P_2')$, and $(P_1' - P_2')$ are quantities that can be measured or calculated. It appears, therefore, that the variables $\overline{\rho'^2}$, $\overline{\rho' u'}$, and $\overline{u'^2}$ could be easily determined if any three of the above four equations are used. This was suggested by Corrsin[24] and others using hot-wire anemometry in turbulent flows. However, it has been shown, and is discussed in detail by A. P. Montealegre[25], that the magnitude of $\overline{\rho'^2}$ is very small in comparison to the other two variables. The error in measuring the fluctuating power is about the same magnitude as $\overline{\rho'^2}$ so that the equations are not actually independent. Hence, these small experimental errors affect the value of $\overline{\rho'^2}$ in the equations tremendously, indicating that $\overline{\rho'^2}$ has to be estimated otherwise, and then $\overline{\rho' u'}$ and $\overline{u'^2}$ calculated from equations III-1-1.28 and III-1-1.29.

III-2 Method of Calculation

A special hot-film sensor called an aspirator probe is used to measure concentrations in the flow field. The operating principle is discussed in Chapter IV. The electrical power input to the sensor to maintain it at a constant temperature is proportional to the molecular weight of the gas flowing past it, and thus, a very smooth curve of gas density versus power input can be drawn. This curve is determined

from a previous calibration of the probe for different known mixtures of the two gases. The velocity past the sensor has a negligible effect on the power dissipation. Hence, if P_c be the power input to the sensor, we have

$$P_c = f(\rho) \qquad \text{III - 2 - 1.1}$$

differentiating the above equation and assuming that a small change on P_c, i. e. dP_c is the fluctuating power p_c, and that similarly $d\rho = \rho'$, we have

$$p_c = \frac{\partial f(\rho)}{\partial \rho} \cdot \rho' \qquad \text{III - 2 - 1.2}$$

Squaring both sides of equation III-2-1.2 and averaging, we have

$$\overline{p_c^2} = \left[\frac{\partial f(\rho)}{\partial \rho}\right]^2 \overline{\rho'^2} \qquad \text{III - 2 - 1.3}$$

p_c can be measured on an RMS voltmeter and from a graph of P_c versus $\rho, \frac{\partial f(\rho)}{\partial \rho}$ at any ρ can be easily determined. Thus $\overline{\rho'^2}$ can be calculated inside the aspirating probe. With this value of $\overline{\rho'^2}$ we can use equations III-1-1.28 and III-1-1.29 to determine $\overline{\rho' u'}$ and $\overline{u'^2}$.

CHAPTER IV

EXPERIMENTAL

Figure IV.1 shows the experimental setup used to obtain data. Essentially it consists of a 4 foot long, 3/4 inch diameter stainless steel tube mounted coaxially in a 6 foot vertical plexiglass duct of square cross section. A centrifugal blower with its inlet connected to the bottom of the duct pulled the outer stream air through the duct, and metered, constant temperature freon 12 was pressure fed through the 3/4 inch steel tube as the inner jet. Hot-wire anemometers were mounted on a traversing mechanism geared to the duct to traverse the field radially and axially, and their power outputs were controlled by two independent channels and recorded on a digital voltmeter.

Duct and Blower The duct had an 8 inch square cross section and was made from plexiglass 3/4 inch thick. It was divided into three sections and joined by flanges. The flanges were sealed with O-rings to prevent air leakage. The duct corners were backed with aluminum angles secured to it by set screws. The first section, a 24 inch entrance region, was made long enough, to ensure a parallel flow field with just small boundary layer build up, and to damp out large scale turbulence. The second was the mixing section, a 36 inch stretch, where the inner, denser freon stream mixed with the outer air stream. The third and exit section was a 12 inch run stacked with cardboard honeycomb to prevent any swirling of the fluid due to exit effects. In order to obtain a flatter velocity profile in the outer air stream and to eliminate the turbulence and temperature effects of the blower, the outer stream air was sucked through the test section by the blower instead of being blown through. The bottom of the duct was connected to the suction end of the blower by 8 inch diameter sheet metal tubing. The blower, a Buffalo type, GE low pressure drop, high capacity, 15 HP, centrifugal blower had its output controlled by a butterfly valve located just before the inlet end. There was no means of measuring the

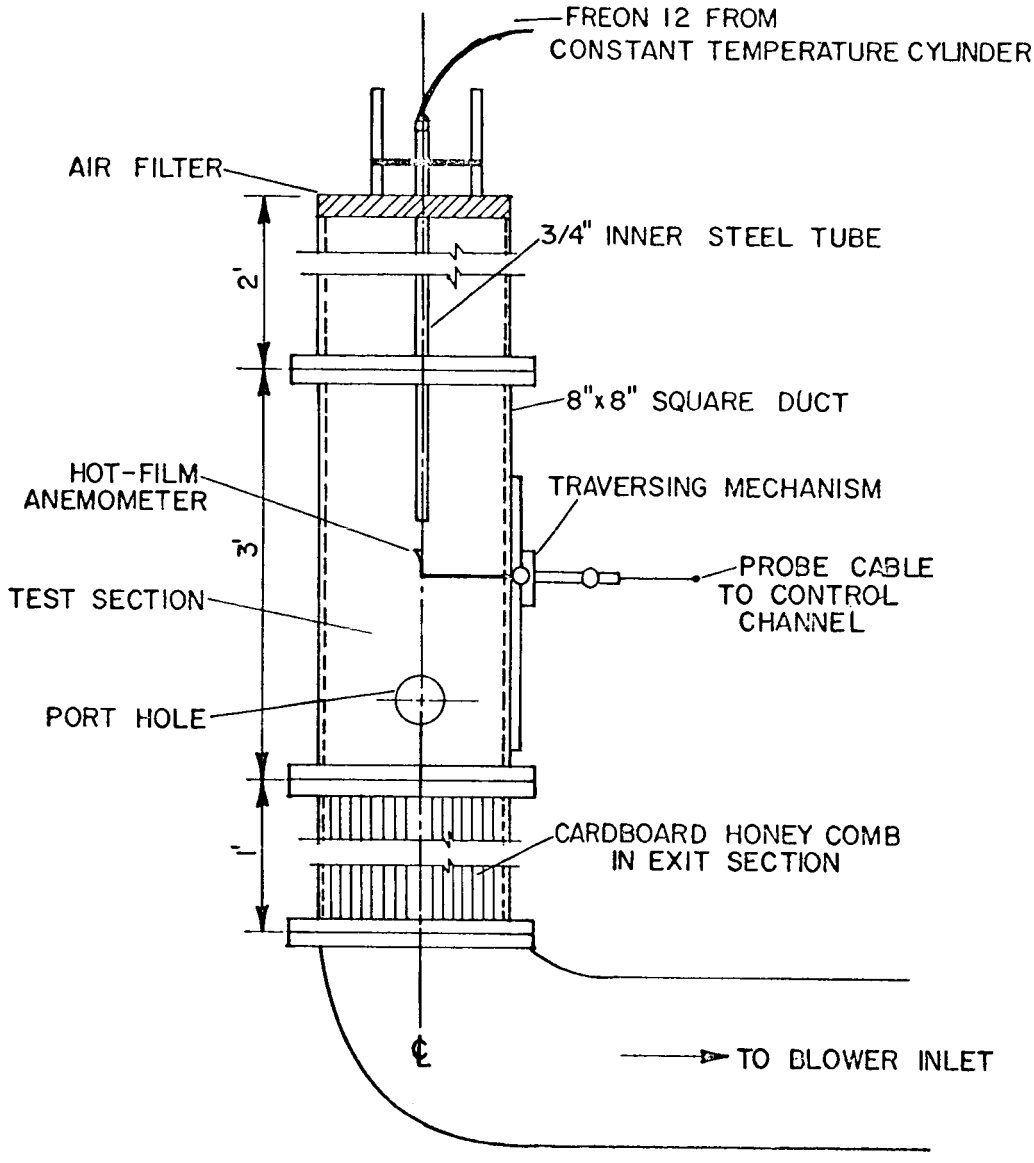

FIGURE IV.1 TEST SECTION

volumetric thruput of the blower, but the outer stream velocity was determined by an anemometer. (The maximum velocity obtained was 56 ft/sec.)

A 24 inch by 1/2 inch slot was milled in the test section of the duct and the traversing mechanism mounted on the duct. The gearing system in the housing permitted radial and axial movement of the probe along a plane containing the axis of the duct. A 4 inch diameter port hole was cut to provide access to the inside of the duct and it was through this that the hot-film anemometers were fixed to the probe holder. An air filter was mounted on top of the duct to prevent fine dust particles in the air from being sucked into the test section and damaging the anemometers. It also served to break up any large eddies.

The 3/4 inch diameter stainless steel tube with a wall thickness of 0.0135 inches was clamped onto a bracket on the duct and checked to be vertical with a plumb bob. A 4 foot length of tubing was needed to insure a fully developed turbulent profile in the tube. Three high precision Brooks rotameters were used to monitor the supply of freon to the inner jet. The rotameters were mounted on a large plywood board along with four pressure gauges and two pressure regulators to control the outlet pressure. The rotameters were selected to allow a wide range of flow rates of the inner stream and could administer from 0.06 SCFM freon 12 to 50 SCFM freon 12 at an outlet pressure of 65 psig within $\pm$ 1% accuracy. For air, the range was 0.1 SCFM to 90 SCFM at an outlet pressure of 40 psig. Small needle valves at the outlet of the rotameters permitted fine regulation of the stream rate.

Freon 12 was obtained from 145 pound cylinders. To compensate for the cooling resulting from vaporization of liquid freon in the cylinder, the cylinders were heated in a large jacketed steam kettle half-filled with water, thus maintaining fairly constant temperature and pressure in the cylinder. The water temperature was maintained around 100°F.

Hot-wire Anemometer System The hot-wire anemometer instrumentation consisting of single wire probes, parallel wire probes, aspirator probes, probe holders, angle adapters, two constant temperature control channels and related monitoring equipment was purchased from Thermo-Systems Incorporated in St. Paul, Minnesota, and was of the constant temperature type. The control channels were independent and each channel could control one sensor. It was possible to monitor either the power input to the sensor or the bridge voltage from the constant temperature control channels. Each unit was equipped with a linearizer that provided a direct measure of power dissipation of the wire. The monitoring equipment included a digital voltmeter, a Hewlitt Packard RMS voltmeter, a sum and difference unit that could add or subtract the outputs from the two independent channels and a dual beam oscilloscope. The power input to the sensor was monitored for calibration and read as a voltage from the digital voltmeter which was directly proportional to the sensor power input. Similarly, the rms value of the fluctuating power input to the sensor was read as an rms voltage directly proportional to the rms power. The dual beam oscilloscope enabled the simultaneous display of two output signals, thus permitting comparison of the signals of separate sensors. It also indicated instability of any sensor on stream.

Most of the sensors used in the experiment were of the hot-film type. The sensor consisted of a thin film of platinum on a quartz cylinder. The hot film sensors were larger in diameter than the hot wires and were more durable and stable. For the experiment two probes were used: (a) parallel wire probe (b) aspirator probe. In the parallel wire probe a 2 mil (0.002") film and a 0.15 mil (0.00015") wire were mounted 0.01 inches apart, parallel to each other on a single probe. The wires were oriented in a plane perpendicular to the plane of the traversing mechanism and were connected to the probe holder by a ninety degree angle adapter. The sensors were, therefore, in a flow field with no external interference.

The aspirator probe was a concentration measuring device and consisted of a 1 mil sensor mounted inside an 0.08 inch ID tube. The tube was connected to an angle adapter and then to the probe holder. The tube contained a jewel bearing with a hole diameter of 0.008 inches $\pm$ 0.001 inch behind the film. A vacuum pump sucked through the probe holder and could sufficiently reduce the pressure downstream from the bearing to insure sonic velocity at the throat of the bearing. This sonic velocity depended on the molecular weight of the gas and therefore, on the composition. The power dissipated at the film would depend on composition and the velocity of the gas passing through; but the velocity past the film could be related to the sonic velocity by the equation of continuity, and since this depended on concentration, the power dissipated from the film could be related to concentration. The device withdrew only a small sample from the stream as would any other concentration measuring device, but provided instantaneous readings at the point of interest.

Calibration of the Hot-film Anemometers - Equipment The calibration section consisted of a 15 foot length of 2 inch diameter schedule pipe with its exit end enclosed in a 6 inch x 6 inch plexiglass chamber 36 inches long. This chamber prevented convection currents in the room from causing any disturbance to the flow pattern in the pipe. A traversing mechanism was mounted on this chamber, and it permitted only vertical movement of the probe. Lateral alignment had to be done by moving the pipe or chamber. A gas mixing section prior to the calibrating section achieved perfect mixing of the air and freon streams, and the gas issuing from the test section was tested to show a homogeneous mixture. The device was made up of three two-inch pipe couplings with two inch to one inch bushings at each end. The couplings and bushings were connected in series by one inch nipples. A two-inch tee with bushings was connected to one of the end couplings. The three couplings and the tee were packed with copper scouring pads. The air and freon streams entered through separate ends in the tee and then passed through the three couplings

in series before entering the test section. The test section was chosen to be long enough to insure fully developed laminar or turbulent profiles.

Constant temperature freon 12 was supplied from heated freon cylinders, mentioned earlier, and the air was taken from a compressed air line. The air was scrubbed and filtered before entering the rotameter. The Brooks high accuracy rotameters metered accurate flow rates of air and freon to the mixing device. A diagram of the flow pattern is shown in figure IV.2.

Procedure Before making any measurements, calibration procedures were established to determine relations between output of the hot-film sensor and gas concentration and velocity. A calibration for the pure air case was obtained first. For a laminar velocity profile it was assumed that the centerline velocity or maximum velocity is twice the average velocity. Air at various laminar flow rates was admitted through a rotameter to the calibrating section and for each flow rate, a single hot-film sensor in the pipe registered the maximum power dissipated. This was read off the digital voltmeter in millivolts. The point of maximum velocity indicated by the sensor was always on or about the centerline of the pipe assuring good profiles. The power dissipated from the hot film was plotted against the square root of the maximum velocity and a linear relationship was obtained. With a hot film, thus calibrated, and able to determine any air velocity, a check on the assumption that the maximum velocity was twice the average velocity was made. A complete velocity profile across a section of the pipe was determined and integrated across the radius to obtain the average velocity. This average velocity compared within three percent to the average velocity set by the rotameter. Care was taken to always keep the air past the sensor at a velocity greater than 1 ft/sec while calibrating, as at velocities below this, free convection plays a significant role in the heat transfer from the hot sensor and the sensor equations have to be modified to include this phenomenon.

In the turbulent region a relationship between maximum velocity in the pipe

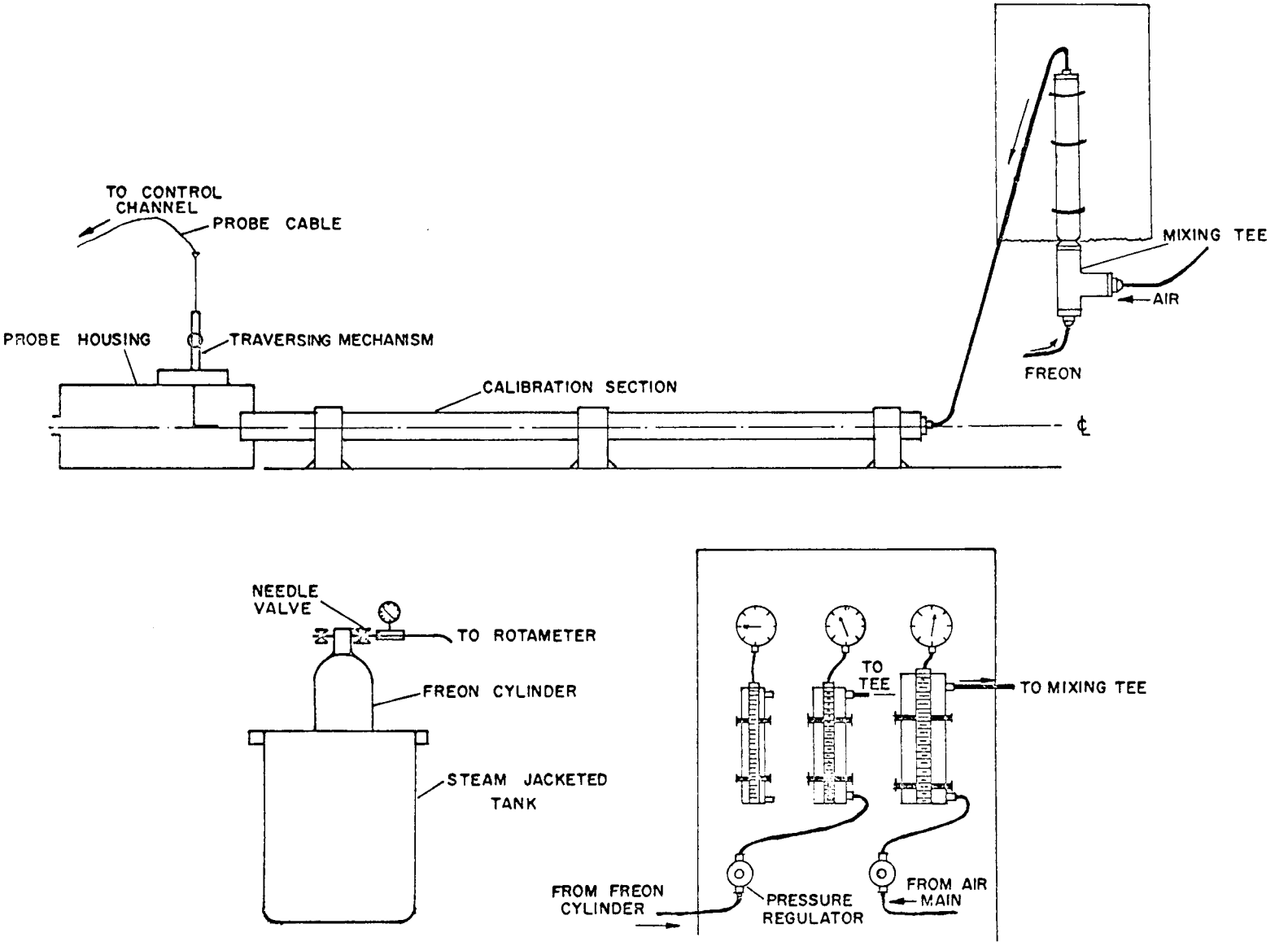

FIGURE IV.2 CALIBRATION SET UP

and average velocity indicated by the rotameter was required. It was not possible with the three high accuracy rotameters to produce gas mixtures of required concentrations and still remain in the laminar region. Thus, sensors were to be calibrated at known turbulent velocities. Two assumptions were made here: (1) the turbulence introduced had no effect on the average measurement; (2) the ratio of average velocity to maximum velocity was only a function of the Reynolds number. A calibrated sensor was introduced into the calibrating section and air velocities at various Reynolds numbers in the turbulent region metered through the rotameters. For each case, the maximum power dissipated by the sensor was converted to a velocity and, knowing the average velocity from the rotameter, a ratio of average velocity to maximum velocity ($U_{avg} : U_{max}$) calculated. A plot of U_{avg} / U_{max} versus Reynolds Number for the 2 inch sch. 40 pipe is shown in figure IV.3. With this relationship of U_{avg} / U_{max} for Reynolds Numbers up to 50,000, the sensor was calibrated for freon air mixtures of 0.1, 0.2, 0.4, 0.5, 0.6, 0.8 and 1.0 mole percent freon. For each of the concentrations the power dissipated by the sensor was found to be linear with the square root of the velocity. Calibration curves of power input versus square root of velocity were obtained for pure air, pure freon, and six other intermediate concentrations. Two typical calibration curves are shown in figure IV.4. Calibration curves for each of the wires in the parallel wire probe were thus obtained.

As was discussed before, the power input to the hot-film in the aspirating probe was dependent only on the molecular weight of the gas and hence obtaining a relation between gas density and power input to the film was rather straight forward. Freon 12 and air were metered through the rotameters to give eight different gas mixtures varying from pure air to pure freon. The aspirator probe was introduced into the test pipe and the vacuum pump turned on. The digital voltmeter read the sensor input in millivolts. The input was found to be constant across the entire pipe

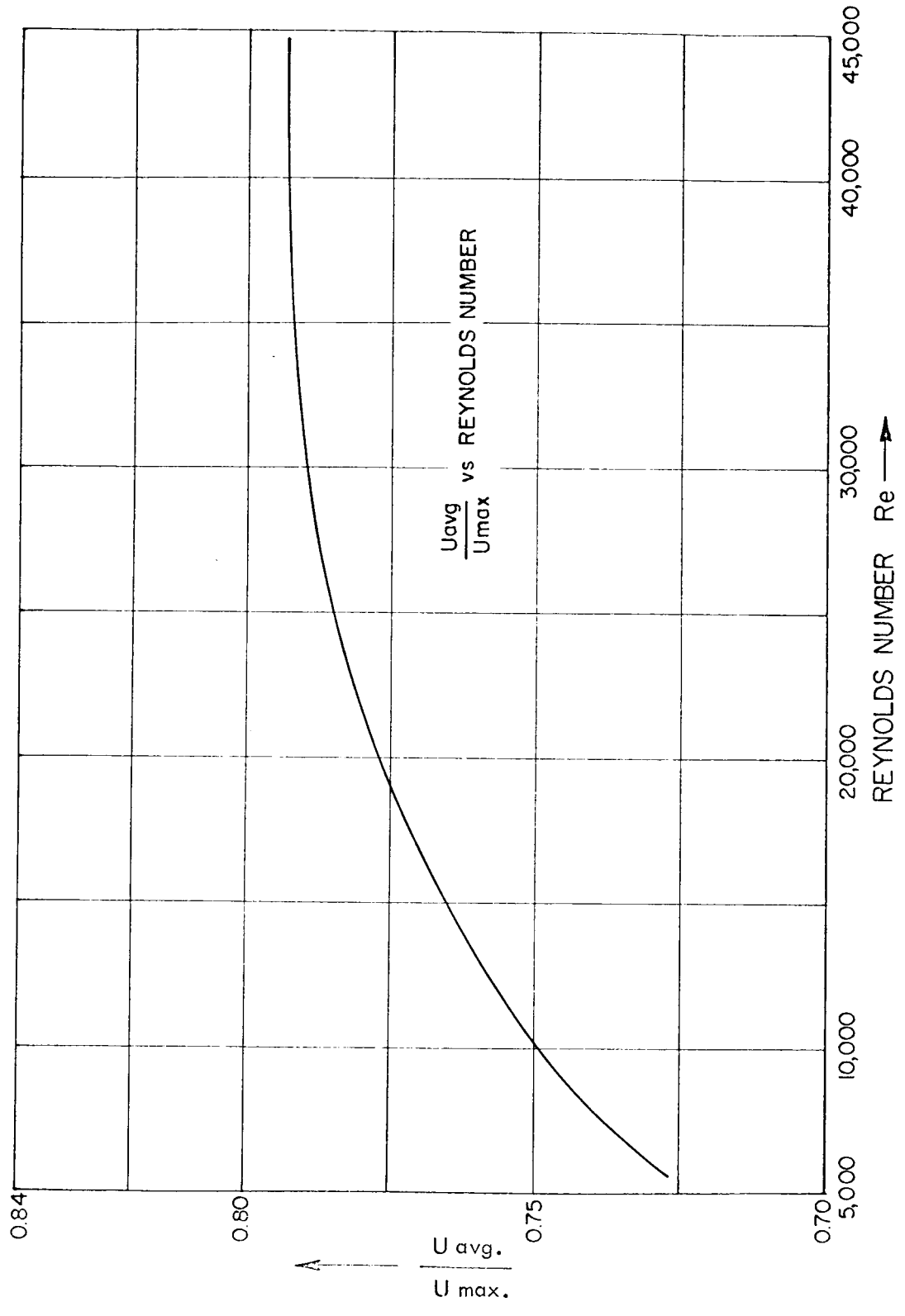
Uavg / Umax vs REYNOLDS NUMBER
0.84
0.80
0.75
0.70
5,000
10,000
20,000
30,000
40,000
45,000
REYNOLDS NUMBER Re
U avg. / U max.

FIGURE IV.3

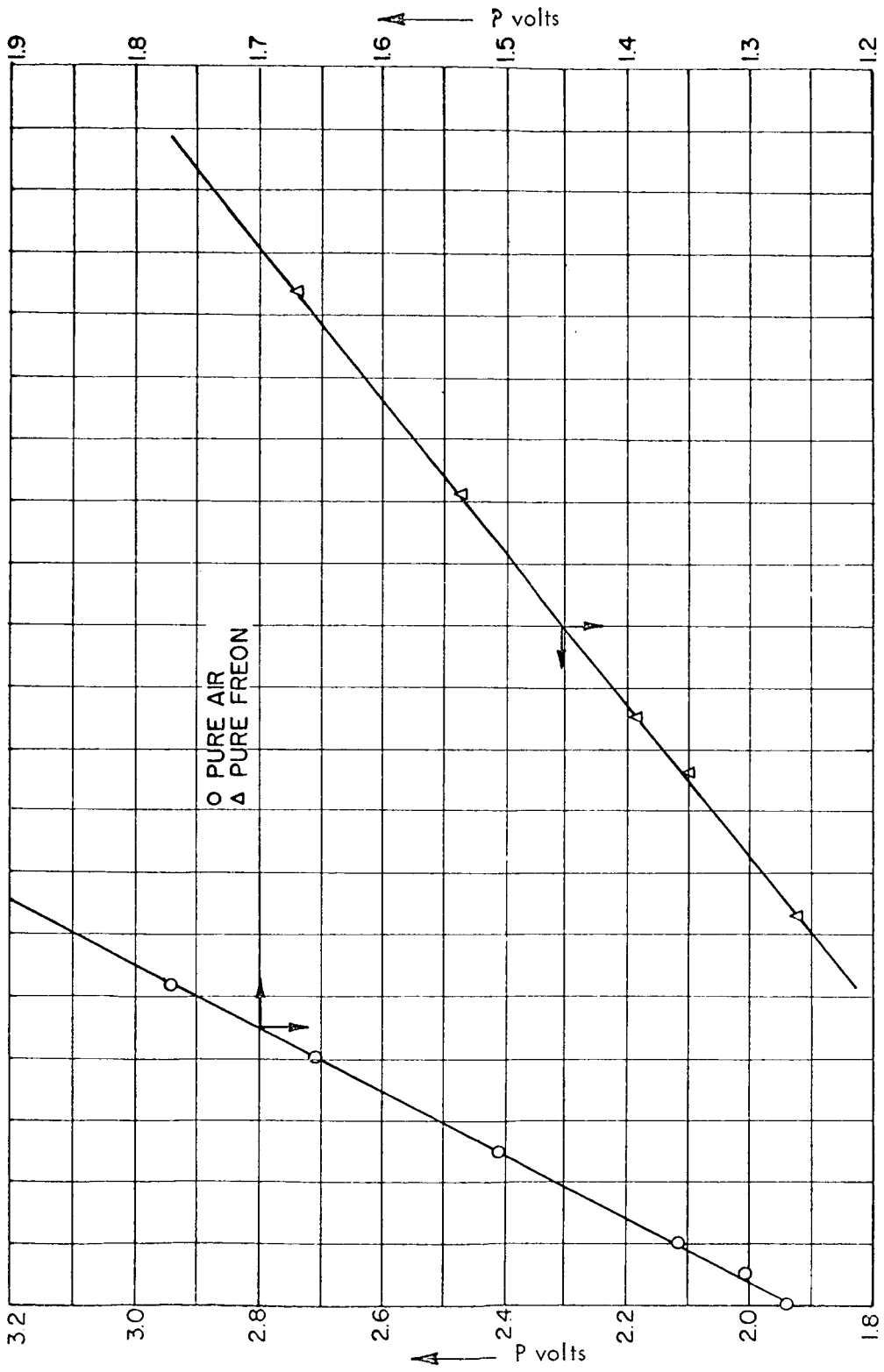

FIGURE IV.4 CALIBRATION CURVES

cross-section indicating complete homogenity. A graph of millivolts registered versus gas density was drawn and shown in figure IV.5.

Experimental Procedure A set of data for a particular inner stream to outer stream velocity ratio included four runs:

1. A run with the aspirator probe to determine density profiles; the aspirator probe was introduced into the test section through the port hole and connected to the holder. It was then taken up to the mouth of the 3/4 inch diameter stainless steel pipe and centered. A diameter of the probe tube was made tangent to the outer circumference of the steel pipe and the probe was then moved in 3/8 inch onto the centerline. The probe was moved downstream on the centerline and was aligned with the initial position by a cathetometer. The signal from the probe was transmitted to the digital voltmeter and the average power input to the probe recorded. The required freon flow rate was set by the rotameter, the blower and the vacuum pump turned on and various positions in the flow field were probed. The data provided a mapping of the average density field for the flow system.
2. A second run with the signal from the aspirator probe connected to the RMS voltmeter gave fluctuating density measurements.
3. The third run was made with a parallel wire probe. Only a 2 mil film was used and the average power supplied to the film was recorded. The data was used to determine average velocity profiles.
4. For the fourth run the outputs from the 2 mil and 0.15 mil wires were transmitted to the RMS voltmeter and the fluctuating voltage recorded.

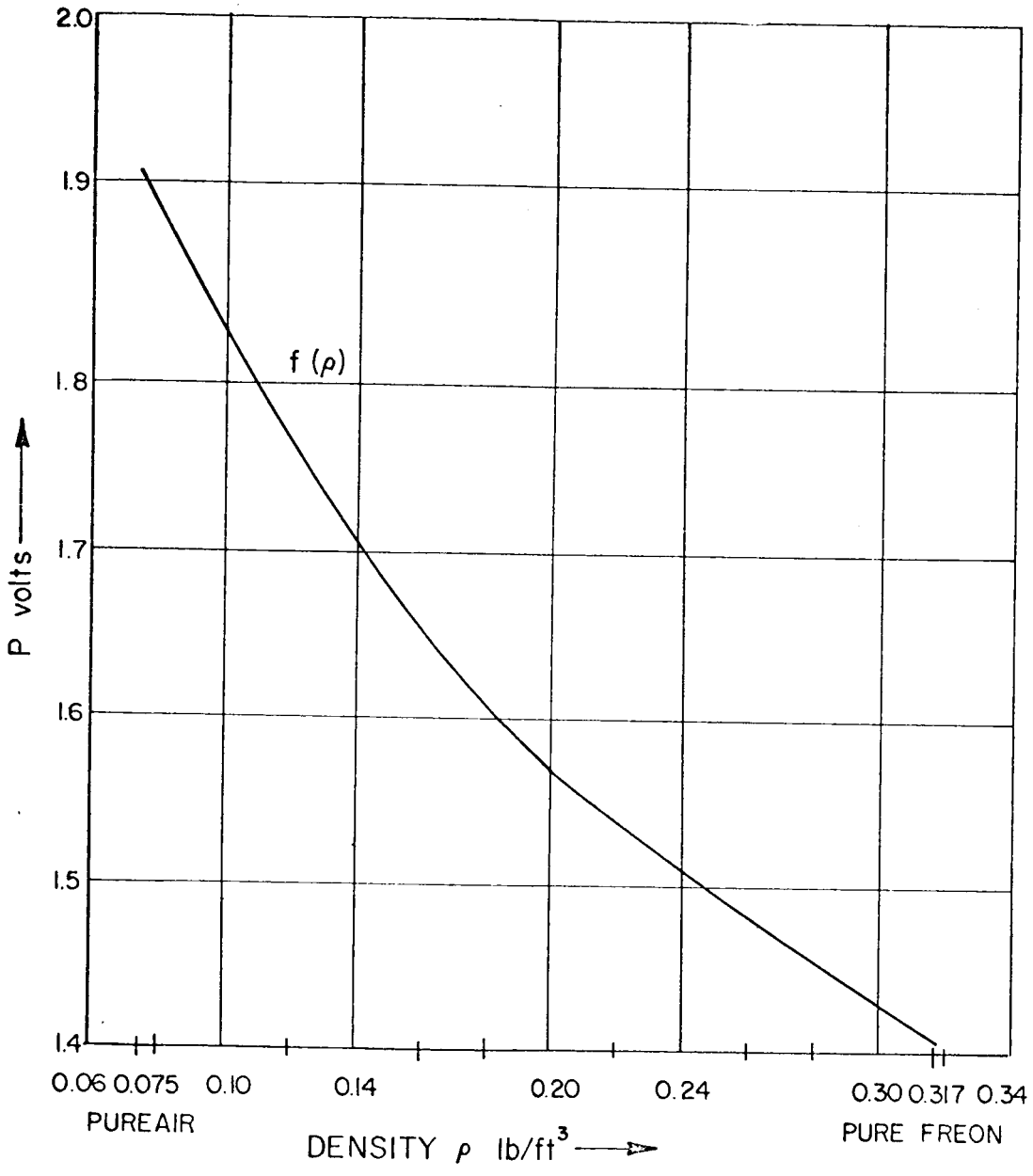

FIGURE IV.5 ASPIRATOR PROBE CALIBRATION CURVE

CHAPTER V

CALCULATION PROCEDURES

The following calibration curves were required for processing the experimental data:

(a) Calibration curve for the aspirator probe-- a relation between power input and density;

(b) Power versus square root of velocity graphs for various freon-air gas mixtures, for both wires on the parallel wire probe;

(c) Subsequent 'A' versus density and 'B' versus density curves as shown in figure V.1.

The power input to the aspirator probe was directly converted to density from the calibration curve (a). A polynomial function representing the power versus density curve was formulated and then the derivative at any density was easily determined. From equation III-2-1.3, we have

$$p_c^2 = \left[\frac{\partial f(\rho)}{\partial \rho}\right]^2 \cdot \rho'^2$$

p_c was the rms voltage to the aspirator probe, and $\frac{\partial f(\rho)}{\partial \rho}$ at various densities was calculated by taking the derivative of the polynomial at those densities. Thus $\overline{\rho'^2}$ in the aspirator probe was determined.

To determine the velocity at a point in the flow field, the density at that point was required. From the 'A' and 'B' versus density curves (c), the values of A and B were read. With the average power supplied to the 2 mil sensor at that point and equation III-1-1.1 ($P = A + BV^{1/2}(T_s - T_e)$), the velocity was calculated.

When the rms signals from the 2 mil film and the 0.15 mil wire were squared and the noise from the sum and difference unit subtracted from them, $\overline{P_1'^2}$

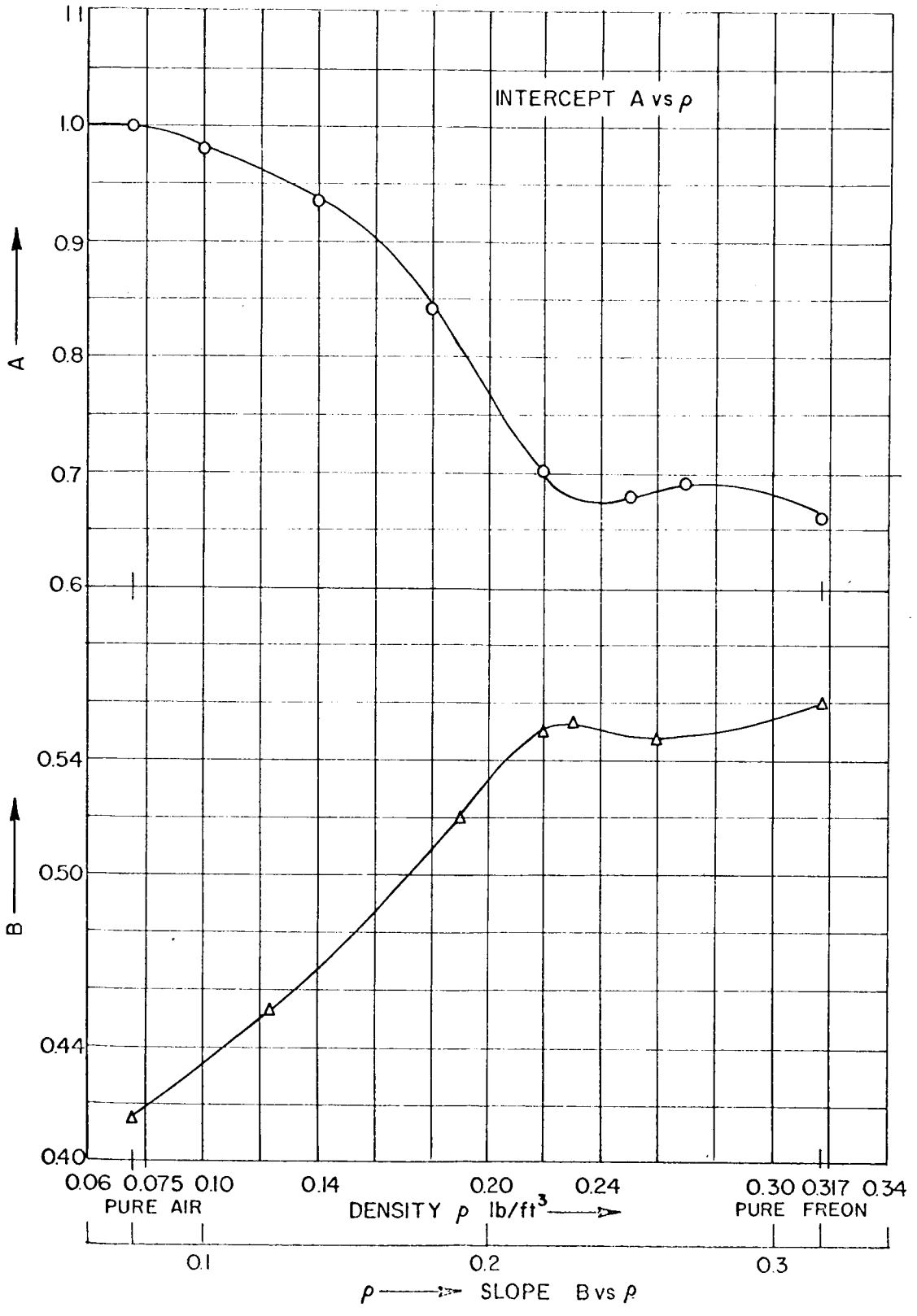

FIGURE V.1 INTERCEPT "A" AND SLOPE "B" VS DENSITY

and $\overline{P_2'^2}$ were obtained for use in equations III-1-1.28 and III-1-1.29. To calculate M_1 and M_2, the quantities $(\frac{\partial A}{\partial \rho})$ and $(\frac{\partial B}{\partial \rho})$ were first evaluated. The A versus ρ and B versus ρ curves for both wires were approximated by 20 degree polynomials and $(\frac{\partial A}{\partial \rho})$ and $(\frac{\partial B}{\partial \rho})$ calculated by taking the derivatives of the polynimial at that density. The coefficients M_1, M_2, N_1 and N_2 were calculated from equations III-1-1.29, III-1-1.20 and III-1-1.22 and equations III-1-1.28 and III-1-1.29 were solved simultaneously.

The fluctuating density $\frac{\sqrt{\rho'^2}}{\overline{\rho}}$, the turbulence intensity $\frac{\sqrt{u'^2}}{\overline{U}}$ and the correlation $\frac{\overline{\rho' u'}}{\sqrt{\rho'^2}\sqrt{u'^2}}$ were subsequently obtained.

A sample calculation for Run 4F is shown below. Axial position 2.0". The concentration profile was first determined with an aspirator probe. The digital voltmeter readings are shown below.

radius 'r'	0"	0.05"	0.1"	0.2"	0.3"	0.4"	0.5"	1.0"
volt read:	1.415	1.422	1.446	1.597	1.759	1.875	1.944	1.944

From a graph of Figure IV.5 these readings were converted to densities.

radius 'r'	0"	0.05"	0.1"	0.2"	0.3"	0.4"	0.5	1.0"
density, ρ lb/ft^3	0.317	0.3095	0.287	0.183	0.121	0.191	0.075	0.075

Figure IV.5 was approximated by a polynomial of the form $1.962 - 1.153\,x + 1.017\,x^2 - 0.396\,x^3$

The quantity $\left[\frac{\partial f(\rho)}{\partial \rho}\right]$ at any density was determined by taking the derivative of the polynomial at that density.

The fluctuating voltage registered by the aspirator probe was used in equation III-2-1.3 to give $\overline{\rho'^2}$

radius r"	0"	0.05"	0.1"	0.2"	0.3"	0.4"	0.5"	1.0"
$(r.ms\ voltage)_{asp}$	0.0086	0.0160	0.0384	0.084	0.0691	0.0475	0 .00225	0.0032
$\frac{\sqrt{\rho'^2}}{\bar{\rho}}$	0.0209	0.0414	0.1133	0.2303	0.1699	0.1225	0	0

The values of 'A' and 'B' in equation III-1-1.1 are determined from graphs as in Figure V.1. With these values and the average voltage recorded by the 2 mil sensor the velocity profile was calculated.

radius:	0"	0.05"	0.1"	0.2"	0.3"	0.4"	0.5"	1.0"
Avg. volt read.	2.530	2.525	2.518	2.674	3.140	3.600	3.870	4.084
'A'	0.6625	0.669	0.685	0.8275	0.962	0.990	1.0	1.0
'B'	0.56	0.5568	0.557	0.511	0.4505	0.427	0.415	0.415
Velocity	11.12	11.11	11.07	13.06	23.37	37.36	47.82	55.22

The fluctuating voltages used in equations III-1-1.28 and III-1-1.29 were:

radius	0"	0.05"	0.1"	0.2"	0.3"	0.4"	0.5"	1.0"
$\overline{P_1'^2}$	.002718	.002954	.004684	.02185	.04156	.0334	.01465	.00188
$\overline{P_2'^2}$	.0002859	.0003312	.0005860	.00425	.006741	.00570	.002498	.000232

The following turbulence intensities were obtained:

radius	0"	.05"	0.1"	0.2"	0.3"	0.4"	0.5"	1.0"
$\frac{\sqrt{u'^2}}{\overline{U}}$	0.0476	0.0508	0.0584	0.2146	0.3401	0.3447	0.0841	0.0277

CHAPTER VI

RESULTS AND DISCUSSION

!. Preliminary Discussion

In highly turbulent flows it has been shown (26) that hot-wires anemometer measurements tend to be inaccurate. For the constant temperature variety this is less predominant. High radial turbulence intensity ($\frac{\sqrt{v'^2}}{\overline{U}}$) also alters the initial equations of the hot-wire and correction factors should be included. This is discussed in detail by Zawacki[3], who has shown, for the homogeneous co-axial compound jet, that the radial turbulence intensity is within the limit and that the measurements were good for the system concerned. It is therefore not illogical to assume that under very much the same experimental setup measurements in the flow field of the heterogeneous compound jet are also good.

While experimental measurements of $\frac{\sqrt{u'^2}}{\overline{U}}$ along the flow field have been made it is assumed that because of the low net radial velocity this turbulence intensity is about the same as the turbulence intensity along the axis.

It has been mentioned before that whereas the fluctuating density measurements ($\frac{\sqrt{\rho'^2}}{\overline{\rho}}$), made with the aspirator probe, were definitely damped and the resulting correlation $\frac{\overline{\rho'u'}}{\sqrt{\rho'^2}\sqrt{u'^2}}$ therefore meaningless, the axial turbulence intensities $\frac{\sqrt{u'^2}}{\overline{U}}$ obtained by the simultaneous solution of the equations III-1-1.28 and III-1-1.29 are valid.

On the assumption that the density fluctuations measured were damped, the density fluctuations determined by the aspirator probe were increased by steady amounts and the values of the corresponding correlations and the axial turbulence intensities calculated; everything else being the same. It was observed that an increase in the density fluctuation of 150% barely changed the turbulence intensity by 8%. It was also observed that while the correlation would have an impossible

value initially, subsequent values obtained by increasing $\overline{\rho'^2}$ were definitely possible. A more extensive discussion of this behavior is given by Montealegre[25] but an excerpt from the results is presented below.

Run No. 4F	Axial Position: 2.0"	Radial Position: 0.2" (from C.L.)
Measured $\frac{\sqrt{\rho'^2}}{\overline{\rho}}$	$\frac{\overline{\rho'u'}}{\sqrt{\rho'^2}\sqrt{u'^2}}$	$\frac{\sqrt{u'^2}}{\overline{U}}$
0.2303	- 1.0060	0.2146
$\frac{\sqrt{\rho'^2}}{\overline{\rho}}$	$\frac{\overline{\rho'u'}}{\sqrt{\rho'^2}\sqrt{u'^2}}$	$\frac{\sqrt{u'^2}}{\overline{U}}$
0.2999	- 0.8624	0.2168
0.3999	- 0.7711	0.2209
0.4999	- 0.7399	0.2260
0.5999	- 0.7361	0.2322

In terms of percentages; when $\frac{\sqrt{\rho'^2}}{\overline{\rho}}$ was changed from 23.03% to 60.0% $\frac{\sqrt{u'^2}}{\overline{U}}$ changed from 21.46% to 23.22%. The correlation with an obviously erroneous initial value of - 1.006 gradually assumed a possible value as the density fluctuations were increased. This is a definite indication that the density fluctuations were damped. It should be noted that all the other calculations exhibited essentially the same lack of dependence of $\overline{\rho'^2}$ and $\overline{u'^2}$.

II. Results

Runs 1F and 2F were taken at high air-freon velocity ratios. Run 1F was at a velocity ratio of 36.8 with an absolute outer stream air velocity of 51.1 ft/sec. Figures 1F.1, 1F.2 and 1F.3 represent the average density, average velocity and turbulence intensity profiles on dimensionless plots. The density profile was plotted as $\frac{\bar{\rho} - \rho_{air}}{\rho_{freon} - \rho_{air}}$ vs r/r_o where $\bar{\rho}$ is the local density, ρ_{air} is 0.075 lb/ft^3, ρ_{freon} is 0.317 16/ft^3, r is the radial position off the center line in inches and r_o the mean tube radius is 0.356". The velocity $\frac{\bar{U}}{U_o}$ was similarly plotted against r/r_o $\bar{U}$ is the local average velocity and U_o the outer stream air velocity.

At axial positions 1/4" and 1/2" a peculiarity in the density profile was observed, an increase in density at r/r_o = 0.6. This phenomena had been detected by Zawacki[3] also, but no explanation is yet available. Run 2F was taken at a velocity ratio of 26.5. Figure 2F.1 and 2F.2 are similar to those of Run 1F.

The profiles in Figures 1F.3 and 2F.3 show a maximum turbulence intensity of about 70% at 1.0" downstream. These maxima, were close to the center line and were very different from the other profiles. At 1/4" and 1/2" the profiles peaked to within 50% at r/r_o = 0.84. These peaks were narrow and they gradually widened, at 2" with a maximum near 30%, to flatter similar looking profiles at 4", 6", and 10" with a maximum of 15% to 8%. The free stream turbulence intensity is about 3.0%. The double peaked profile in Figure 1F.3 at 1/2" axial distance may be due to the irregular velocity profile at that position. There is no definite explanation justifying this behavior. The boundary layer effect appears to be more pronounced at this axial position and this might have caused the double peaks in the turbulence intensity.

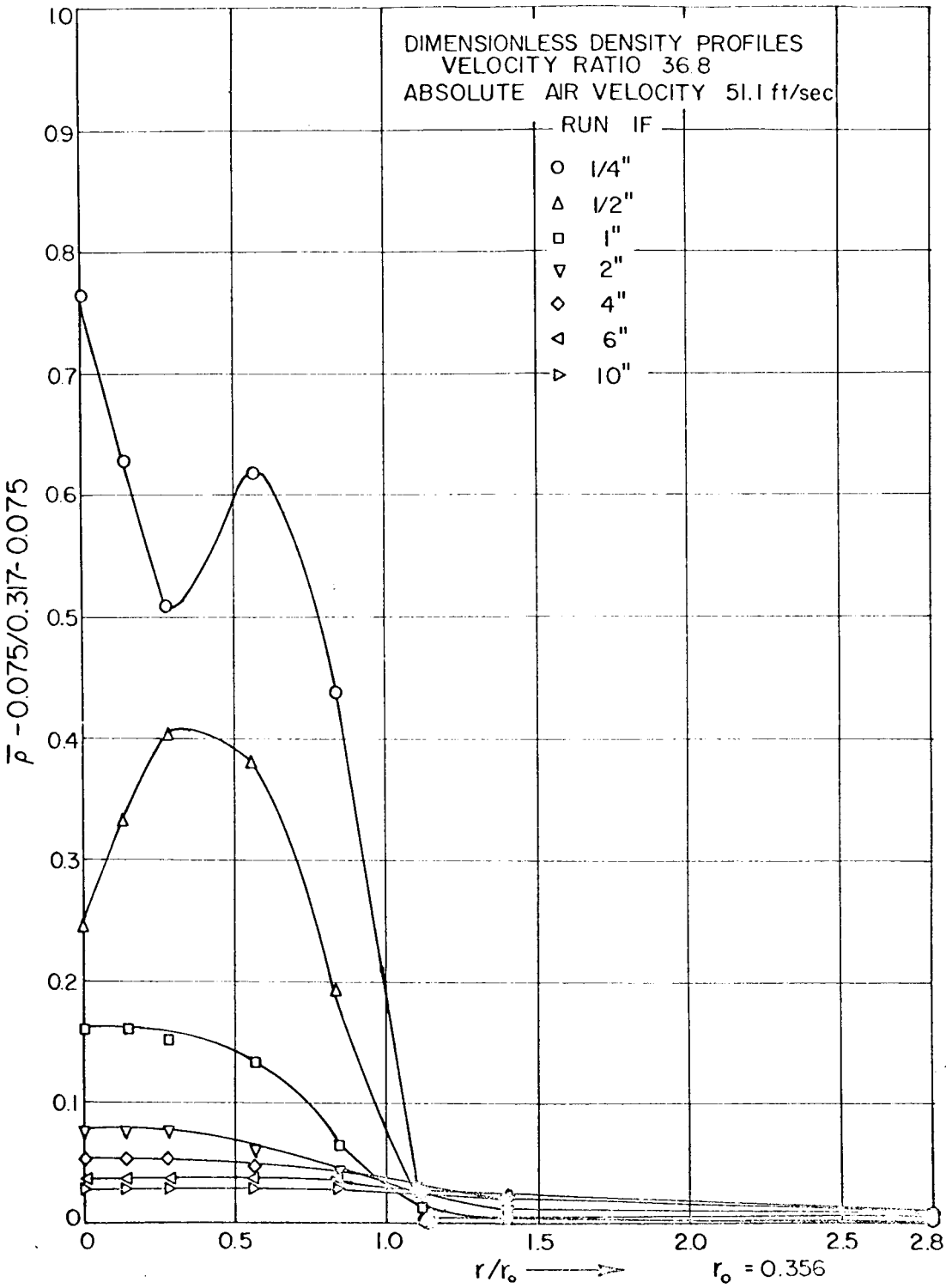
DIMENSIONLESS DENSITY PROFILES
VELOCITY RATIO 36.8
ABSOLUTE AIR VELOCITY 51.1 ft/sec
RUN 1F
1/4"
1/2"
1"
2"
4"
6"
10"
$\bar{\rho}$ - 0.075/0.317 - 0.075
r/r$_o$
r$_o$ = 0.356
0
0.1
0.2
0.3
0.4
0.5
0.6
0.7
0.8
0.9
1.0
0.5
1.0
1.5
2.0
2.5
2.8

FIGURE 1F.1

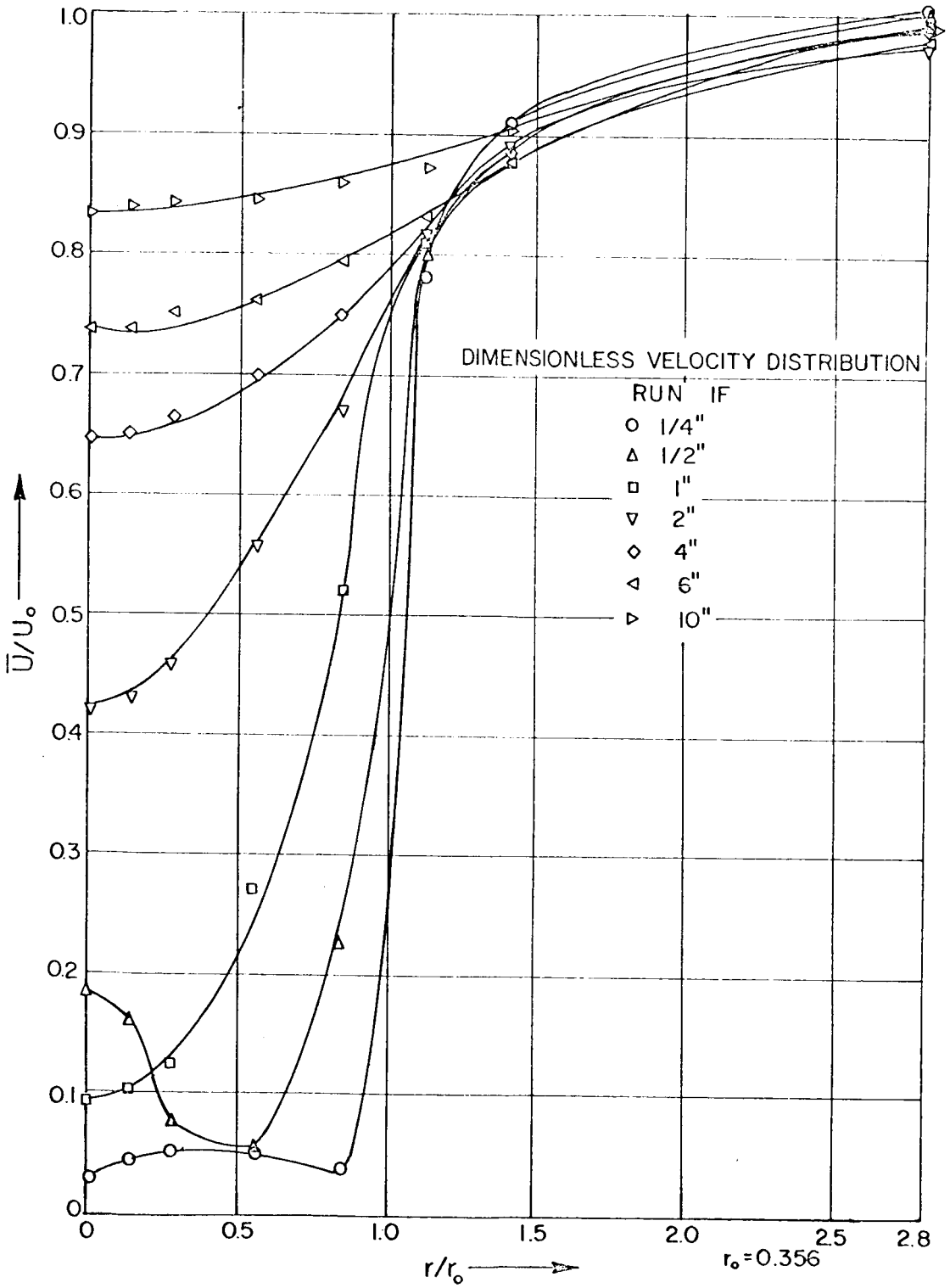
DIMENSIONLESS VELOCITY DISTRIBUTION
RUN IF
1/4"
1/2"
1"
2"
4"
6"
10"
$\bar{U}/U_o$
r/r_o
$r_o = 0.356$
1.0
0.9
0.8
0.7
0.6
0.5
0.4
0.3
0.2
0.1
0
0.5
1.0
1.5
2.0
2.5
2.8

FIGURE 1F.2

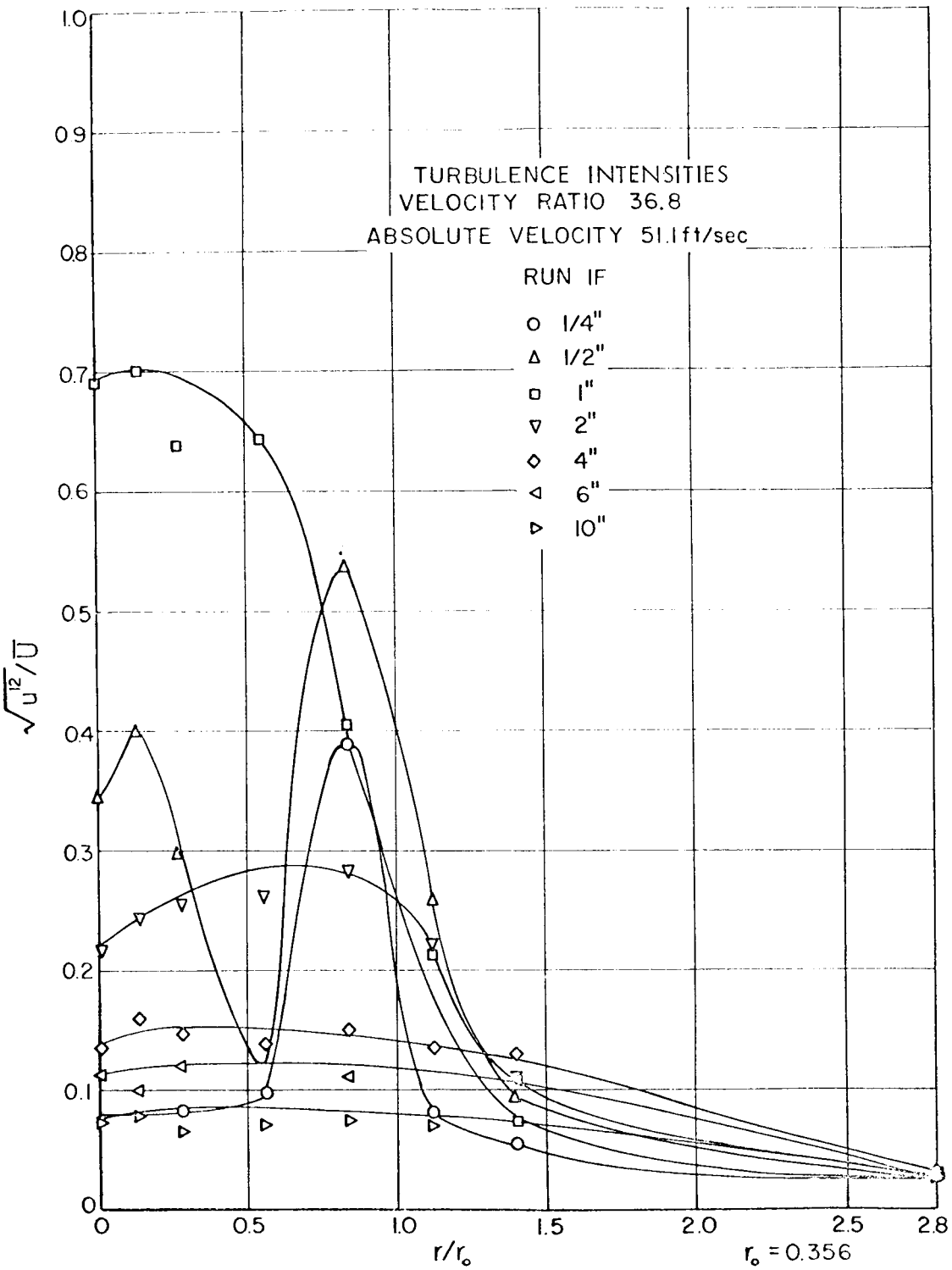
TURBULENCE INTENSITIES
VELOCITY RATIO 36.8
ABSOLUTE VELOCITY 51.1 ft/sec
RUN 1F
1/4"
1/2"
1"
2"
4"
6"
10"
$\sqrt{u'^2}/\bar{U}$
r/r_o
$r_o = 0.356$
0
0.1
0.2
0.3
0.4
0.5
0.6
0.7
0.8
0.9
1.0
0.5
1.0
1.5
2.0
2.5
2.8

FIGURE 1F.3

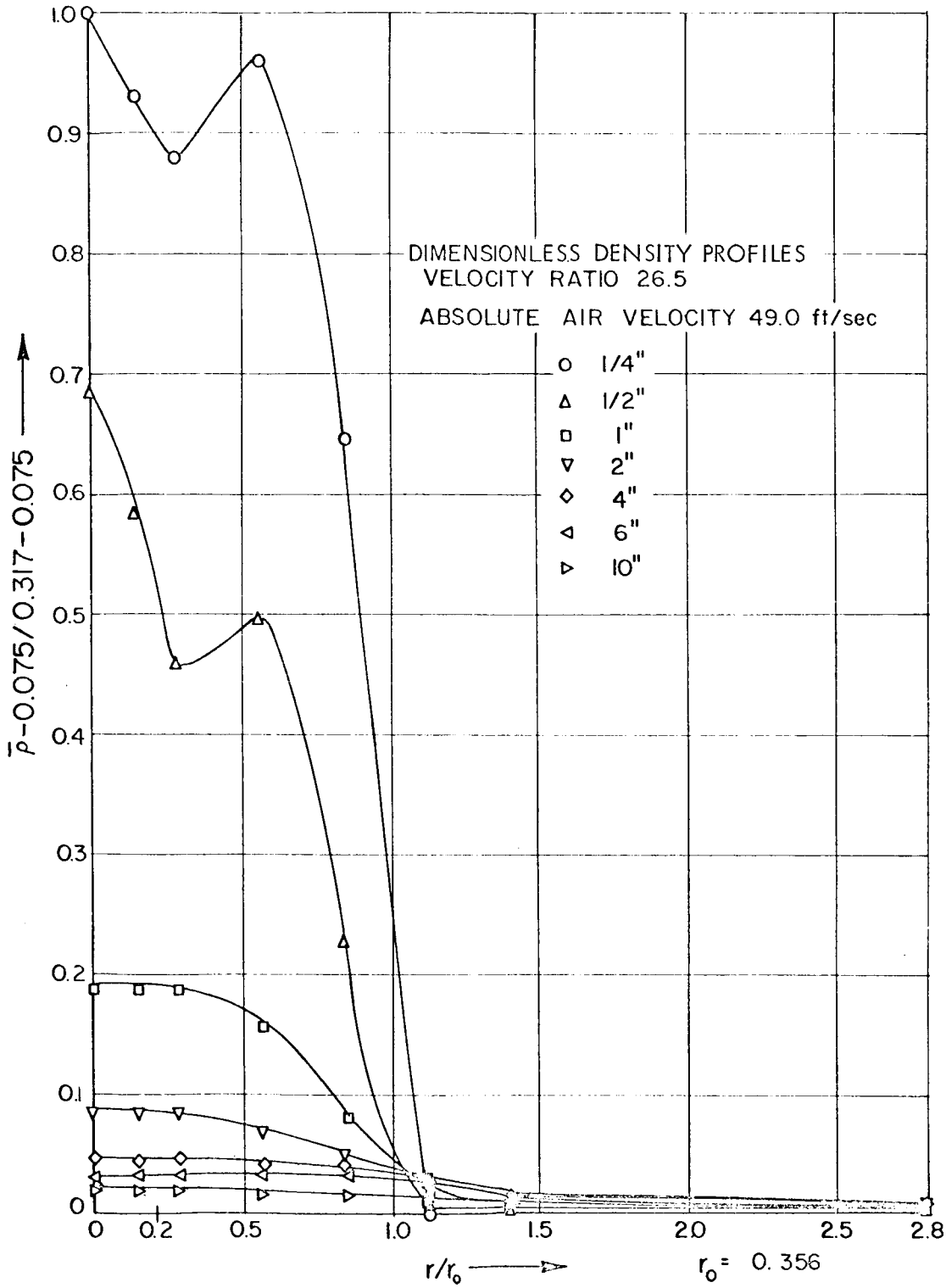
DIMENSIONLESS DENSITY PROFILES
VELOCITY RATIO 26.5
ABSOLUTE AIR VELOCITY 49.0 ft/sec
1/4"
1/2"
1"
2"
4"
6"
10"
$\bar{\rho}$-0.075/0.317-0.075
r/r$_o$
r$_o$ = 0.356
1.0
0.9
0.8
0.7
0.6
0.5
0.4
0.3
0.2
0.1
0
0
0.2
0.5
1.0
1.5
2.0
2.5
2.8

FIGURE 2F.1

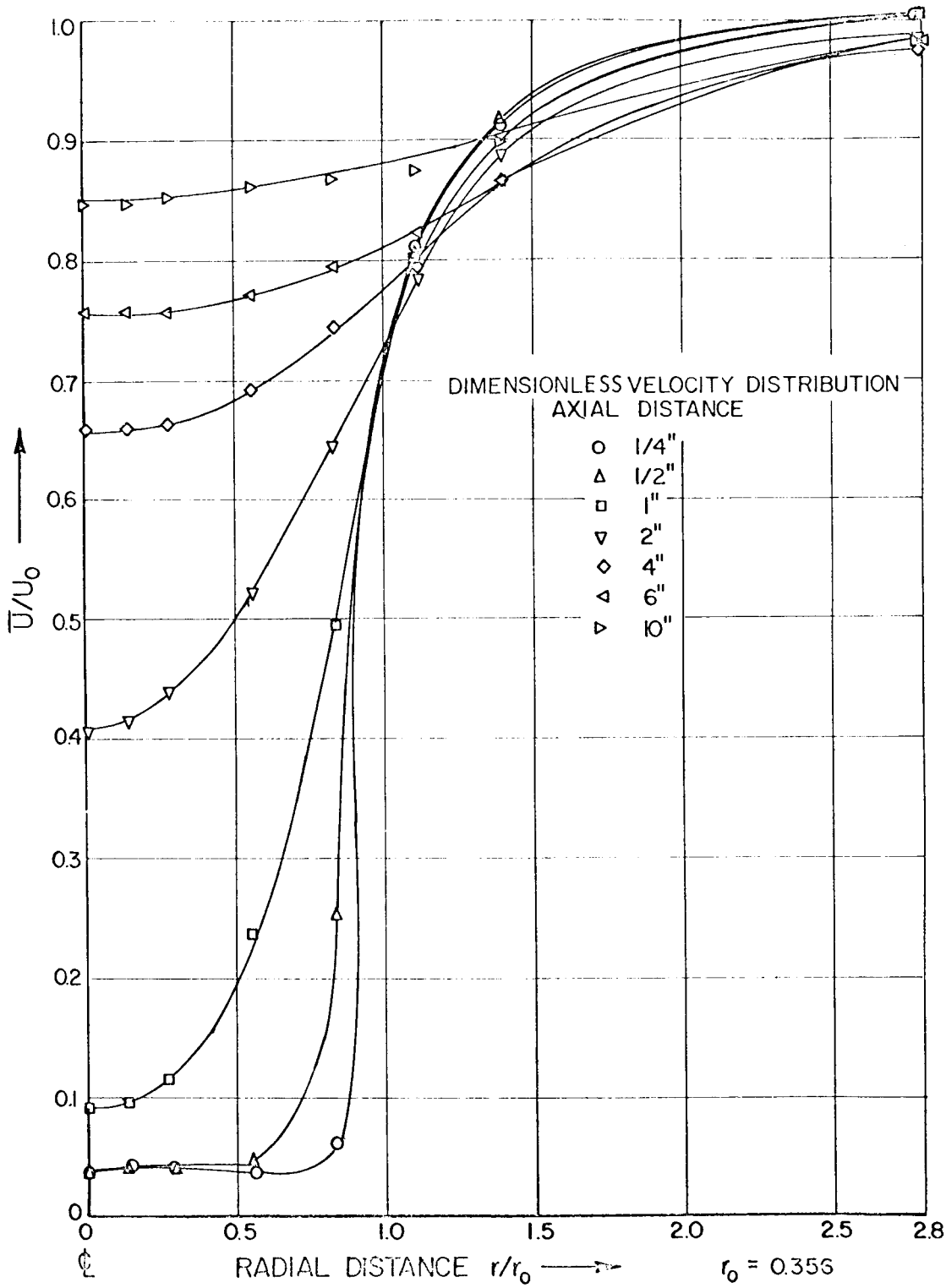
DIMENSIONLESS VELOCITY DISTRIBUTION
AXIAL DISTANCE
1/4"
1/2"
1"
2"
4"
6"
10"
$\bar{U}/U_o$
RADIAL DISTANCE r/r_o
r_o = 0.356
1.0
0.9
0.8
0.7
0.6
0.5
0.4
0.3
0.2
0.1
0
0.5
1.0
1.5
2.0
2.5
2.8

FIGURE 2F.2

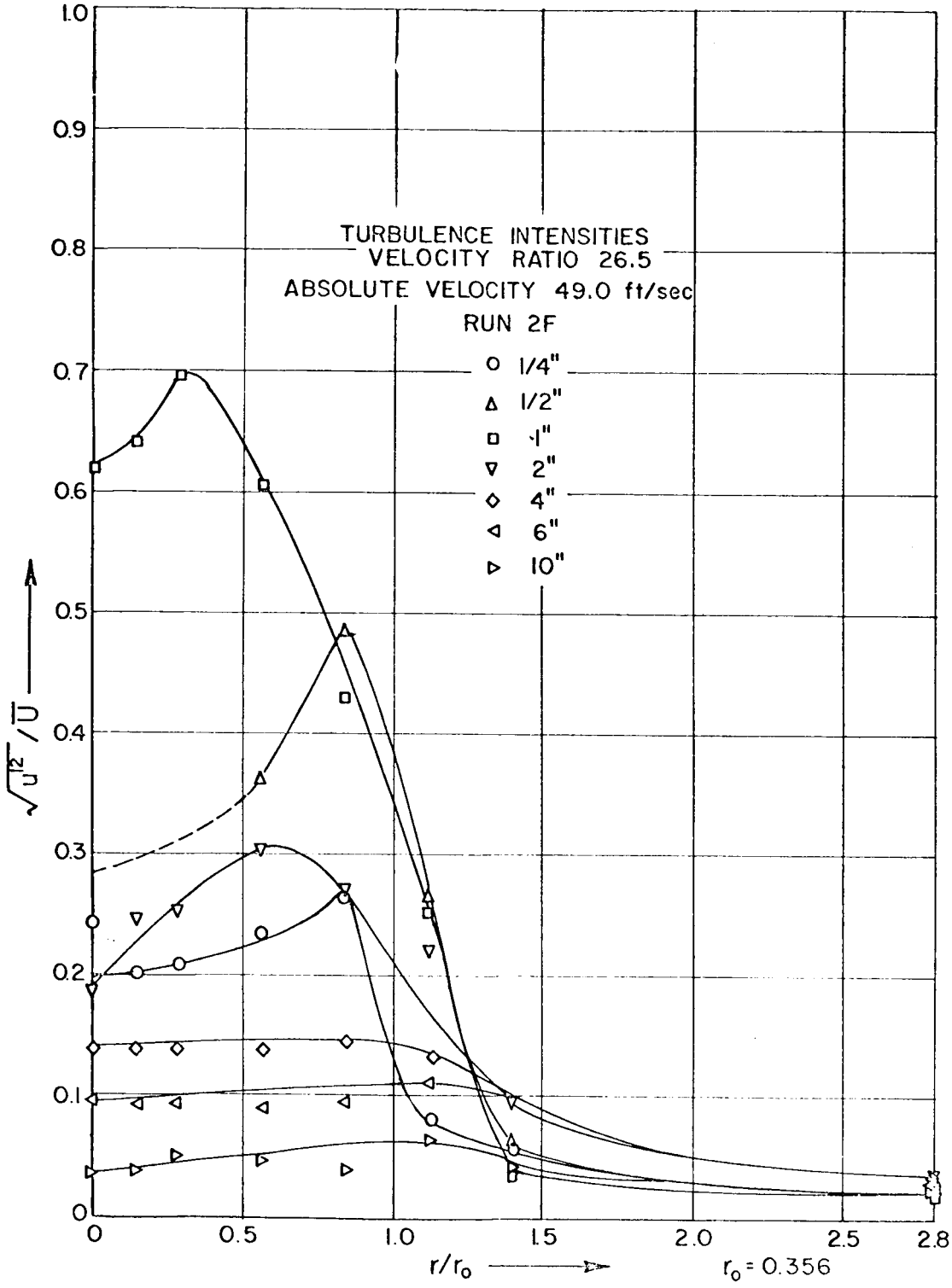
TURBULENCE INTENSITIES
VELOCITY RATIO 26.5
ABSOLUTE VELOCITY 49.0 ft/sec
RUN 2F
1/4"
1/2"
1"
2"
4"
6"
10"
$\sqrt{u'^2}/\bar{U}$
r/r_o
$r_o = 0.356$
0
0.1
0.2
0.3
0.4
0.5
0.6
0.7
0.8
0.9
1.0
0.5
1.0
1.5
2.0
2.5
2.8

FIGURE 2F.3

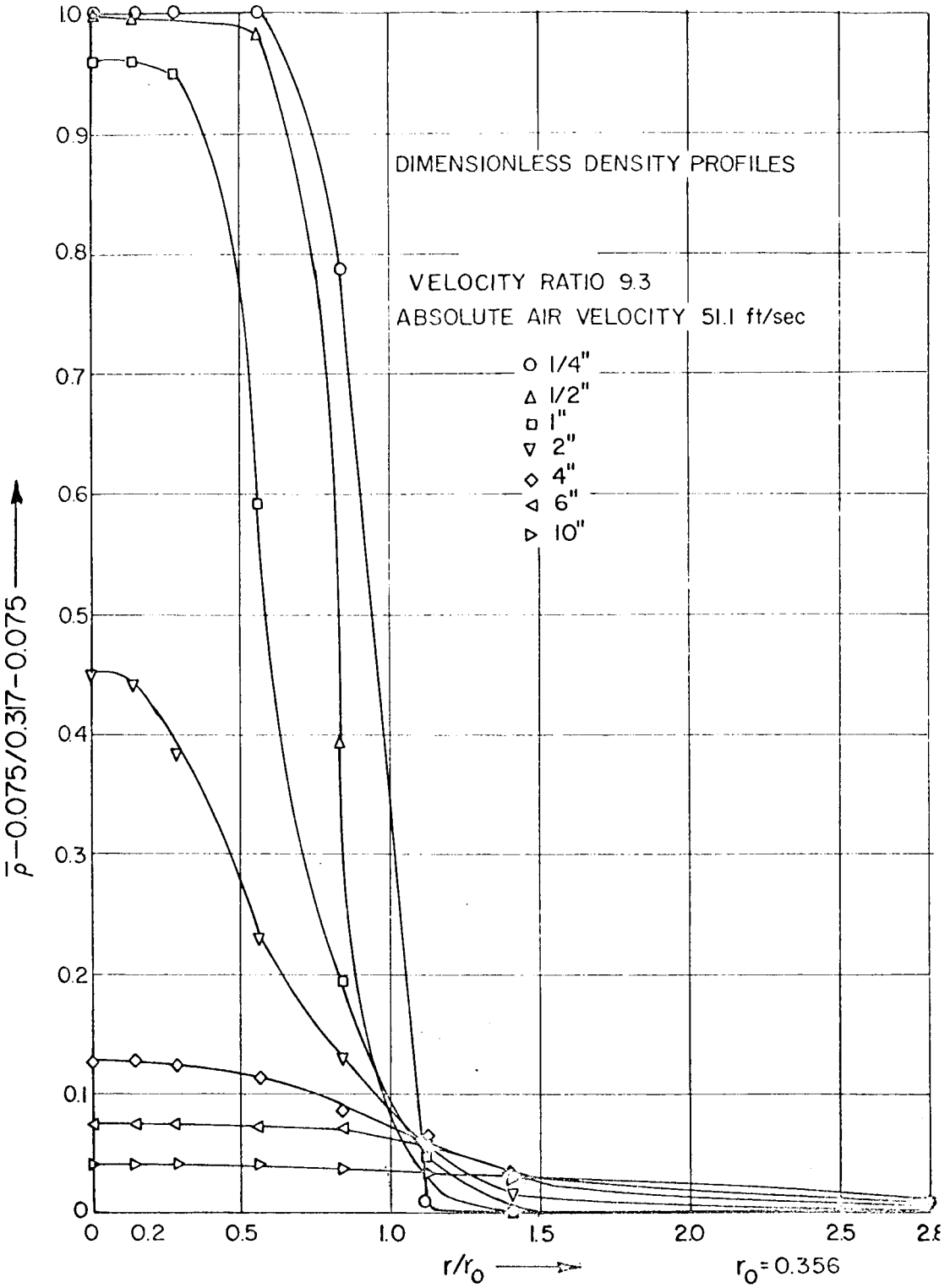
DIMENSIONLESS DENSITY PROFILES
VELOCITY RATIO 9.3
ABSOLUTE AIR VELOCITY 51.1 ft/sec
1/4"
1/2"
1"
2"
4"
6"
10"
$\bar{\rho}$-0.075/0.317-0.075
r/r$_o$
r$_o$=0.356
1.0
0.9
0.8
0.7
0.6
0.5
0.4
0.3
0.2
0.1
0
0.2
0.5
1.0
1.5
2.0
2.5

FIGURE 3F.1

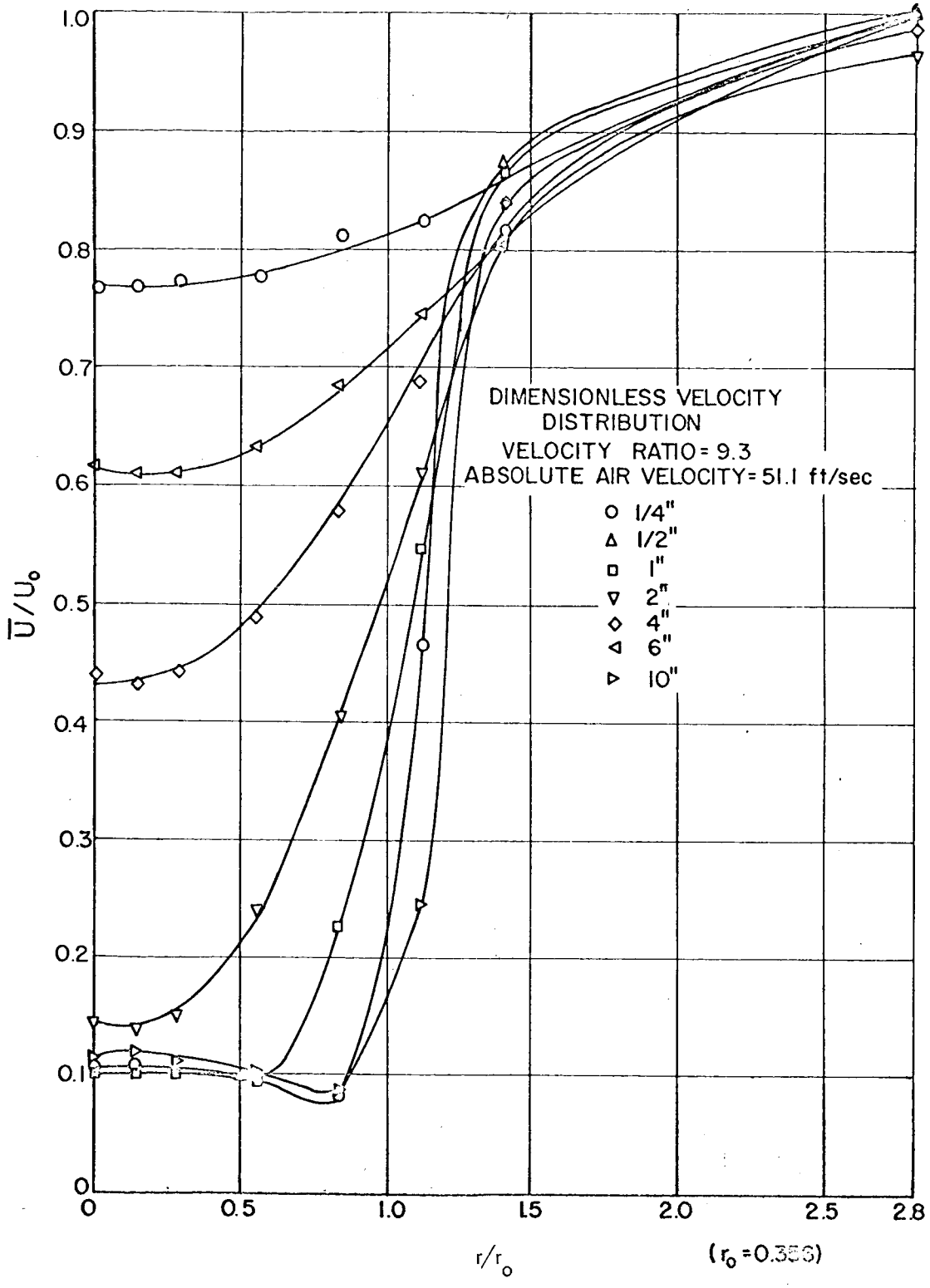
DIMENSIONLESS VELOCITY
DISTRIBUTION
VELOCITY RATIO = 9.3
ABSOLUTE AIR VELOCITY = 51.1 ft/sec
1/4"
1/2"
1"
2"
4"
6"
10"
$\bar{U}/U_o$
r/r_o
(r_o = 0.353)
0
0.1
0.2
0.3
0.4
0.5
0.6
0.7
0.8
0.9
1.0
0.5
1.0
1.5
2.0
2.5
2.8

FIGURE 3F.2

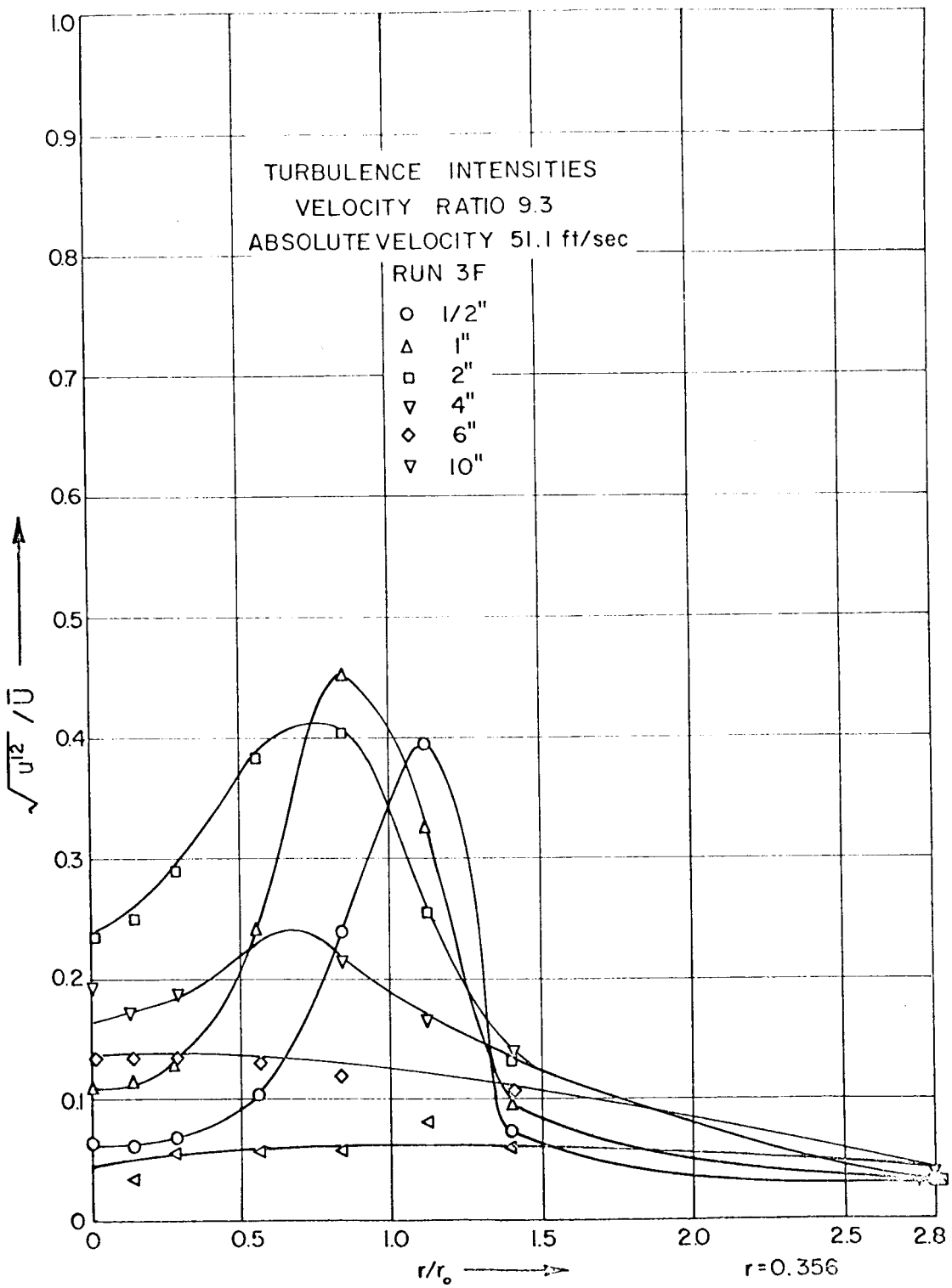
TURBULENCE INTENSITIES
VELOCITY RATIO 9.3
ABSOLUTE VELOCITY 51.1 ft/sec
RUN 3F
1/2"
1"
2"
4"
6"
10"
$\sqrt{u'^2}/\bar{U}$
r/r_o
r=0.356
0
0.1
0.2
0.3
0.4
0.5
0.6
0.7
0.8
0.9
1.0
0.5
1.0
1.5
2.0
2.5
2.8

FIGURE 5F.3

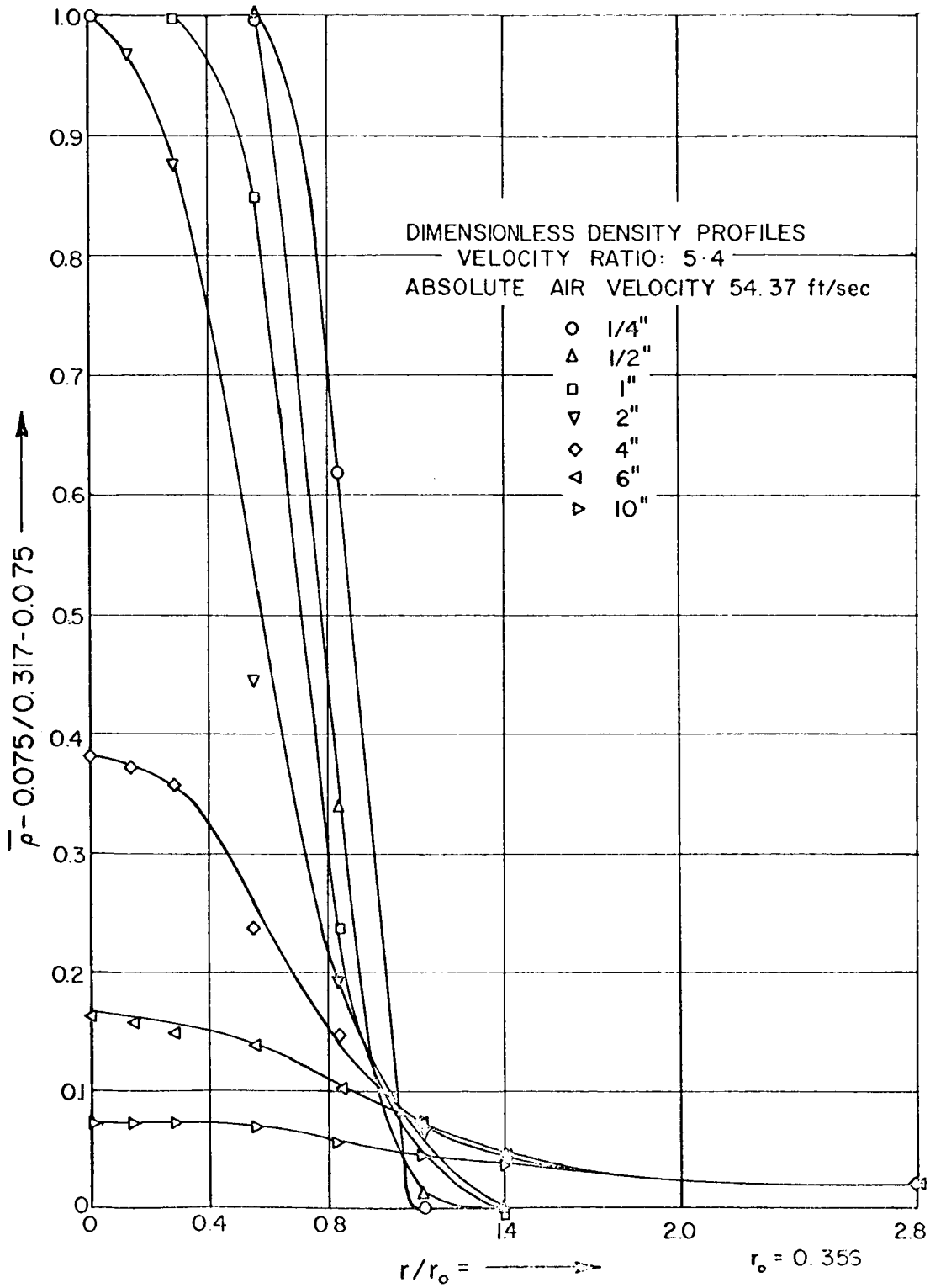
DIMENSIONLESS DENSITY PROFILES
VELOCITY RATIO: 5·4
ABSOLUTE AIR VELOCITY 54.37 ft/sec
1/4"
1/2"
1"
2"
4"
6"
10"
$\bar{\rho}$ - 0.075/0.317-0.075
r/r$_o$ =
r$_o$ = 0.356
1.0
0.9
0.8
0.7
0.6
0.5
0.4
0.3
0.2
0.1
0
0
0.4
0.8
1.4
2.0
2.8

FIGURE 4F.1

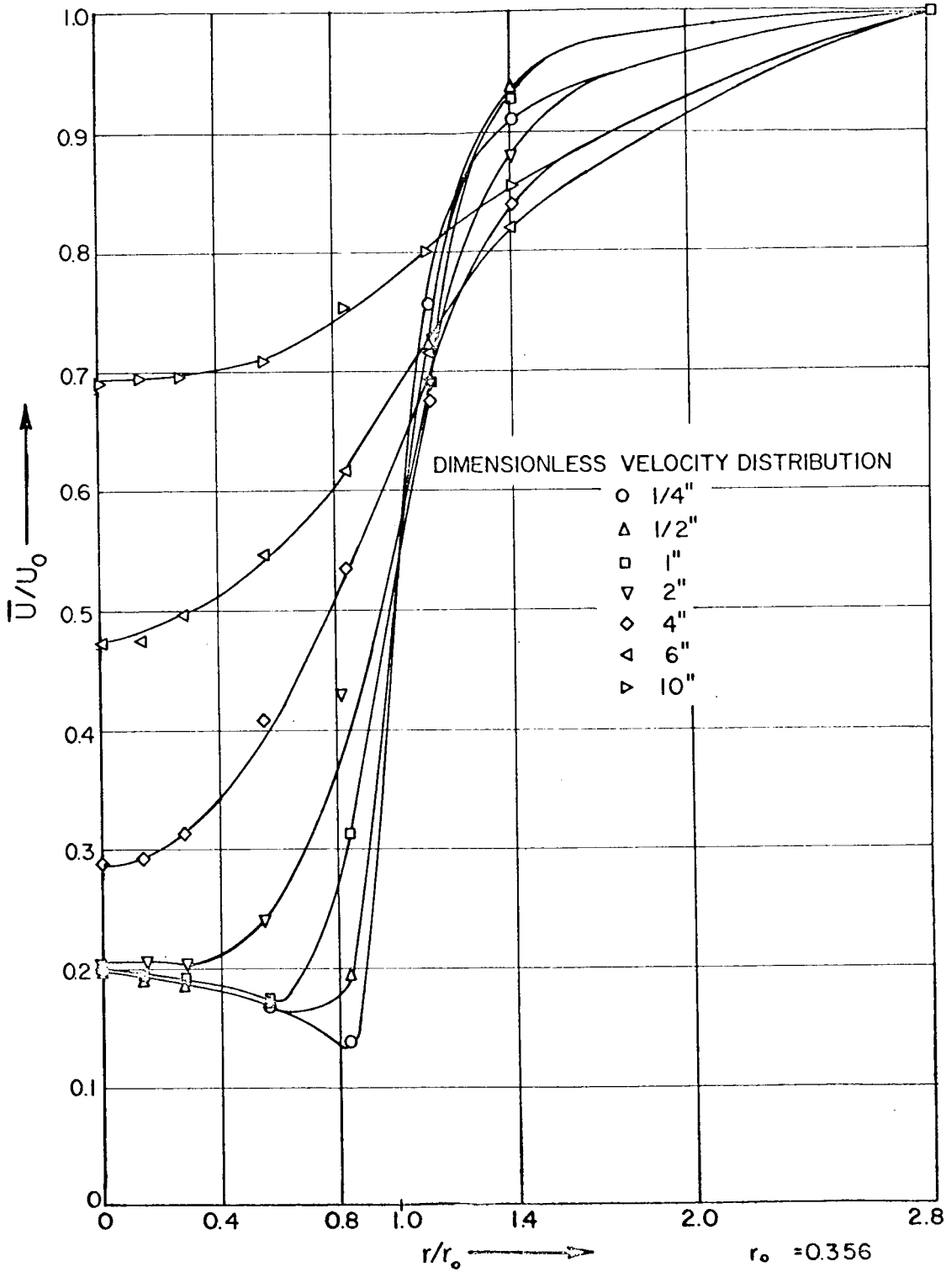
DIMENSIONLESS VELOCITY DISTRIBUTION
1/4"
1/2"
1"
2"
4"
6"
10"
$\bar{U}/U_o$
r/r_o
r_o =0.356
0
0.1
0.2
0.3
0.4
0.5
0.6
0.7
0.8
0.9
1.0
0.4
0.8
1.0
1.4
2.0
2.8

FIGURE 4F.2

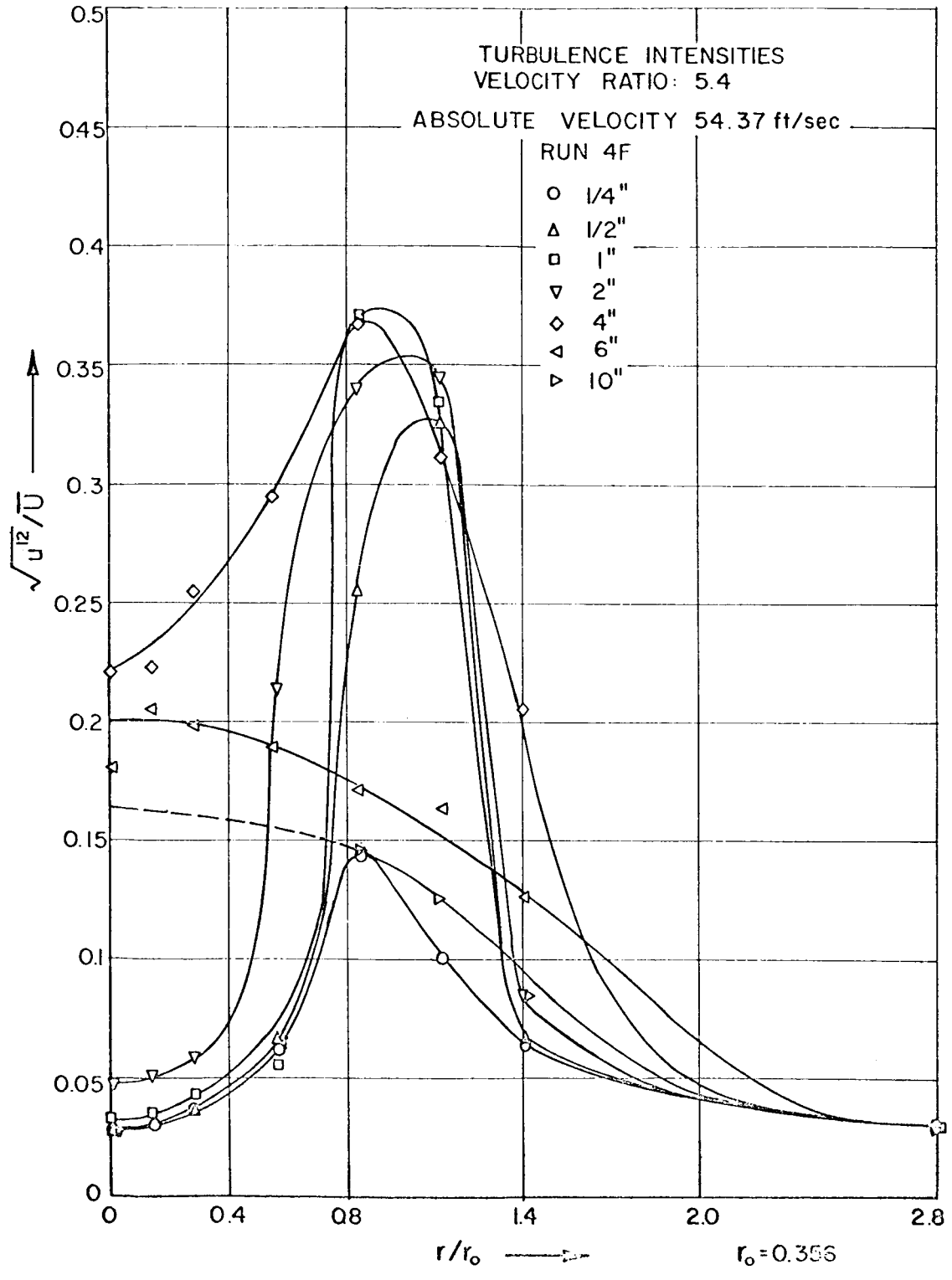
TURBULENCE INTENSITIES
VELOCITY RATIO: 5.4
ABSOLUTE VELOCITY 54.37 ft/sec
RUN 4F
1/4"
1/2"
1"
2"
4"
6"
10"
$\sqrt{u'^2}/\bar{U}$
0.5
0.45
0.4
0.35
0.3
0.25
0.2
0.15
0.1
0.05
0
0
0.4
0.8
1.4
2.0
2.8
r/r_o
$r_o = 0.356$

FIGURE 4F.3

Run 3F and 4F were taken at velocity ratios of 9.3 and 5.4 with absolute air velocities of 51.1 ft/sec. and 54.37 ft/sec. respectively. Density, velocity and turbulence intensity profiles were plotted on the same variables. The density profiles were smooth and at no axial position was the density on the center-line less than the density at any other radial position. The boundary layer effect of the steel tube was easily detected in the velocity profile by a decrease in velocity at $r/r_o = 0.84$. Velocity and density profiles begin to look similar from the 4.0" axial position downwards. This occurs at 1.0" from the high velocity ratio runs. Maximum turbulence intensities for these two cases were about 40.0% to 45.0%. The widening of the peaks and the subsequent flattening of the profiles were also noted in Run 1F and 2F.

The turbulence intensity field could be divided into two main regions. An initial region characterized by high narrow peaking of the profiles and a "similarity" region where profiles were apparently similar. Depending on the velocity ratio these regions occurred at different axial position. For a higher velocity ratio the initial region was restricted to an axial position of 2.0" whereas this extended from 4.0" to 6.0" at the lower velocity ratio cases.

In the region close to the jet opening the data reported may not be very accurate. Because of the nature of the fluctuation it was not always possible to take satisfactory data. Furthermore, in this region a change of $\overline{\rho'^2}$ affected $\overline{u'^2}$ considerably more than in other cases

A comparison of the above reported data with typical turbulence intensity data of Zawacki[3] for the homogeneous jet show a resemblance in the profiles. At small distances downstream the peaks were narrower and the maxima were only as high as 40.0% in Zawacki's data. These maxima occurred at a radial position $r/r_o = 0.84$. The peaks widen with distance from the jet mouth and gradually the profiles look similar. In this similar region the maximum was not so well pronounced

and has a magnitude of about 15%. At high velocity ratios however no high turbulence intensities were observed on the center-line 1" downstream. No double peaks in the intensity profiles were observed.

CONCLUSIONS

The conclusions drawn from this experimental work are:

I. Theoretically it has been indicated that the equations from three independent hot-film anemometers provide a method for determining $\sqrt{\rho'^2}$ $\sqrt{u'^2}$ and $\overline{\rho'u'}$. For the flow system considered it was found that the magnitude of the experimental error in the data is as large as the value of $\overline{\rho'^2}$ and hence the equations were not really independent. Another method to estimate $\sqrt{\rho'^2}$ was necessary.

II. The fluctuating power recorded by the aspirator probe is not a measure of the fluctuating density in the flow field but of that in the aspirator tube. These fluctuations are considerably damped from those in the free stream.

III. Because of the relationship between $\sqrt{\rho'^2}$ and $\sqrt{u'^2}$ a large change in the magnitude of $\sqrt{\rho'^2}$ usually has only a small effect on the magnitude of $\sqrt{u'^2}$.

IV. The turbulence intensity profiles may be divided into an initial region and a similar region, much like the density and velocity profiles.

V. In the initial region intensities are higher than in the similar portion with maxima having magnitudes about 40%. In the similar region intensities are only about 15%. The maximum depends on the velocity ratio of the streams.

VI. There is a similarity between intensity profiles of a homogeneous jet and those of a heterogeneous jet.

BIBLIOGRAPHY

1. Schlichting, H., "Laminare Strahlausbreitung" ZAMM 13, 1933.

2. Andrade, E. N., "The Velocity Distribution in a Liquid into Liquid Jet- The Plane Jet". Proc. Phys. Soc. Lond. 51, 1939.

3. Zawacki, T., Ph. D. Thesis "Turbulence in the Mixing Region of Co-axial Streams". Ill. Inst. of Tech. 1967.

4. Abramavitch, G. N., "The Theory of Turbulent Jets. M. I. T. Press. Cambridge, Mass. 1963.

5. Tollmien, W., "Berechnung Turbulenter Aus breitungsvorgänge" ZAMM 6, 1926 Translated as NACA TM 1085, 1945.

6. Goertler, H., "Berechnung von Aufgaben der freien Turbulenz auf Grund eines neuen Näherungsansatzes" ZAMM 22, 1942.

7. Keuthe, A. M., "Investigation of the Turbulent Region Formed by Jets" Journal of Applied Mechanics, Trans. ASME Vol. 57, 1935.

8. Squire, H. B. and Trouncer, J., "Round Jets in a General Stream" Aeronautical Research Committee Technical Report, R & M No. 1974, 1944.

9. Ferri, A., Libby, P. A. and Zakkay, V., "Theoretical and Experimental Investigations of Supersonic Combustion" Aeronautical Res. Lab. Report ARL 62-467 Sept. 1962.

10. Alpinieri, L. J., "An Experimental Investigation of the Turbulent Mixing of Non-homogeneous Co-axial Jets". Polytech Inst. of Brooklyn, Pibal Rept. 789, 1963, also "Turbulent Mixing of Co-axial Jets AIAA. Journal Vol. 2 1964.

11. Ragsdale, R. G., H. Weinstein and Lanzo, C. D., "Correlation of a Turbulent Air-Bromine Co-axial Flow Experiment".

12. Boehman, L., "Mass and Momentum Transport Properties in Isoenergetic Co-axial Flows", Ph. D. Thesis, Illinois Inst. of Tech. 1966.

13. Weinstein, H. and Todd, C. A., "Analysis of Mixing of Co-axial Streams of Dissimilar Fluids Including Energy Generation Terms.

14. Corrsin, S., Natl. Advisory Committee Aeronaut. Wartime Reports No. 94, 1943.

15. Corrsin, S., and Uberoi, M. S., "Further Experiments in the Flow and Heat Transfer in a Heated Turbulent Jet" NACA Rept. 998, 1950.

16. Tani, I. and Kobashi, Y., "Experimental Studies on Compound Jets" Proceedings of the 1st Japan National Congress for Appl. Mech., 1951.

17. Kobashi, Y., "Experimental Studies on Compound Jets" (measurement of turbulent characteristics) Proceedings of the 2nd Japan National Congress for Appl. Mech. 1952.

18. Rosensweig, R. E., "Measurement and Characterization of Turbulent Mixing Fuels Res. Lab. May, 1959.

19. Blackshear Jr., P. L. and Fingerson, L., "Rapid Response Heat Flux Probe for High Temperature Gases", ARS Journal, Nov.1962.

20. Conger, W. L., "Measurement of Concentration Fluctuations in the Mixing of Two Gases by Hot-wire Anemometer Techniques". Ph.D. Thesis Univ. of Penn. 1965.

21. King, L. V., Phil Trans Roy. Soc. London 214A pg. 273, 1917.

22. Van der Hegge Zijnen, B. G., Appl. Sci. Research 6A pg. 129, 1956.

23. Kramers, H., Physica 12, pg. 61, 1946.

24. Corrsin, S., "Extended Applications of the Hot Wire Anemometer" NACA Technical Note 1864, 1949.

25. Montealegre, A. P. M.S. Thesis, "Evaluation of Turbulent Correlations in a Co-axial Flow"., Ill. Inst. of Tech. 1967.

26. Hinze, J. O., "Turbulence" Mc Graw-Hill Book Co.

NASA-Langley, 1968 —— 12 E-4130